Carnegie Mellon University
Computational Bio-Modeling Lab

Integrated Design Innovation Group

Carnegie Mellon University

Thesis Defense:

A Method to Design Hybrid Lattice Support Structures for LPBF Additive Manufacturing

Lisha White, PhD. Candidate, Carnegie Mellon University

Committee Members:
Dr. Jonathan Cagan[1], Dr. Yongjie Jessica Zhang[1]
Dr. Anthony Rollett[2], Dr. Guanglu Zhang[1]

1. Carnegie Mellon University, Department of Mechanical Engineering
2. Carnegie Mellon University Department of Material Science and Engineering

Additive Manufacturing (AM) of Metals[1]

✓ Pros	− Cons	• Example Techniques
✓ Complex geometry ✓ Mass customization ✓ No specialized tooling	− Initial start-up costs − Limited materials − Build time vs. accuracy	• Directed Energy Deposition • Material Extrusion • Powder Bed Fusion

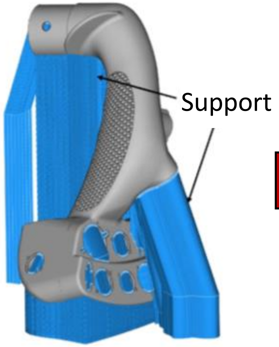

Part to Build[2]

→ AM Metal Technique →

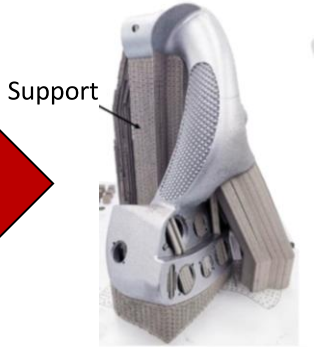

Final Build[2]

1. Vafadar, A., et. al (2021) 2. Wang, D., et.al (2022)

Laser Powder Bed Fusion (LPBF)

Layer-wise addition of material to create a part using a high-power laser to melt metal alloy powder[1]

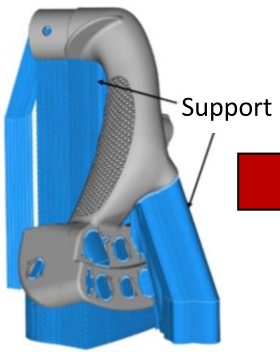

Part to Build[2]

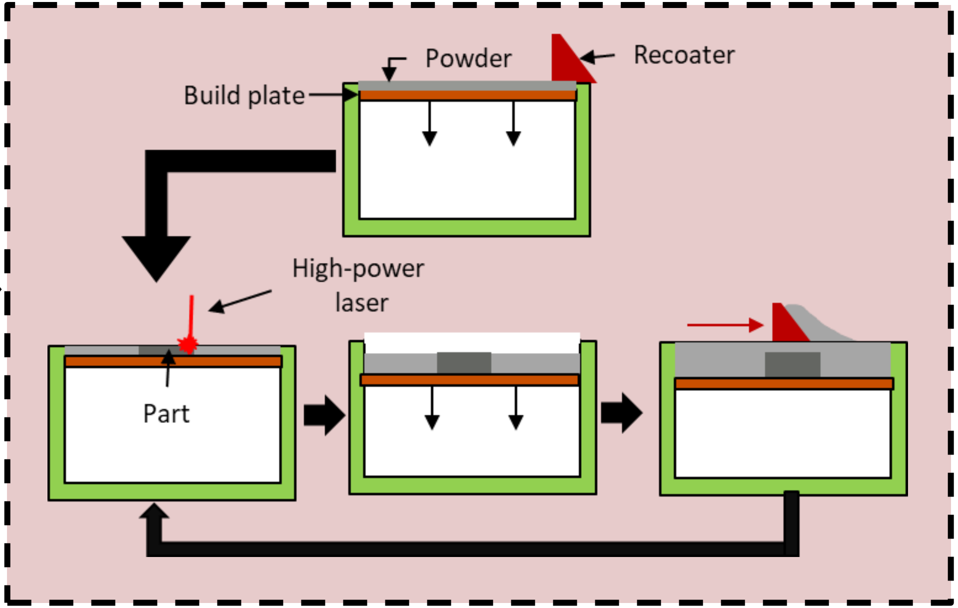

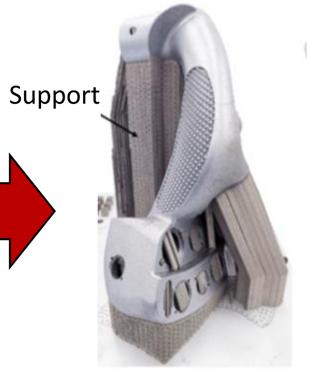

Final Build[2]

1. Vafadar et. al (2021) 2. Wang, D., et.al (2022)

Laser Powder Bed Fusion (LPBF)

Residual Stress

Block shell support[3]

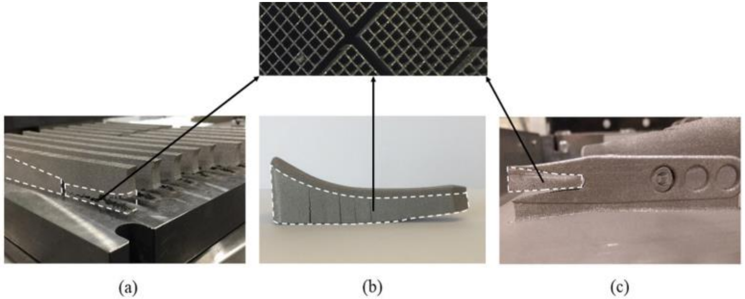

Support Structure Purpose[4,5]:

- **Dissipate Heat**[5,6,7]
- Maintenance of structural integrity[3,8,9]

Lattice Structures for AM

- Individual unit cells distributed to control bulk properties[10,11]

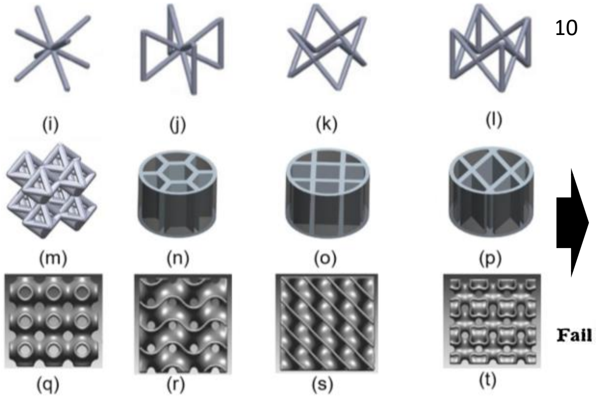

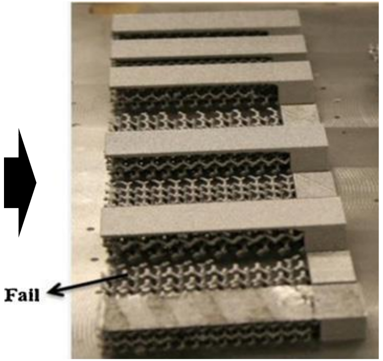

3. Cheng, L., et. al (2019)
4. Jiang, J, et. al (2018)
5. Huang, R., et. al (2020)
6. Bartsch, K., et. al (2019)
7. Lee, K.H., et.al (2022)
8. Bartsch, K., et. al (2018)
9. Pellens, J., et.al (2020)
10. Nazir, A., et. al (2019)
11. Liang, H et. al (2011)
12. Hussein, A., et. al (2013)

Limitations to Lattice Support Structure Design

Gradient-Based Optimizer[13,14]

✓ Ideal for differentiable objective functions

✓ Fast convergence

Optimize density distribution[4,10,11,19]

Minimize thermal gradient w.r.t density

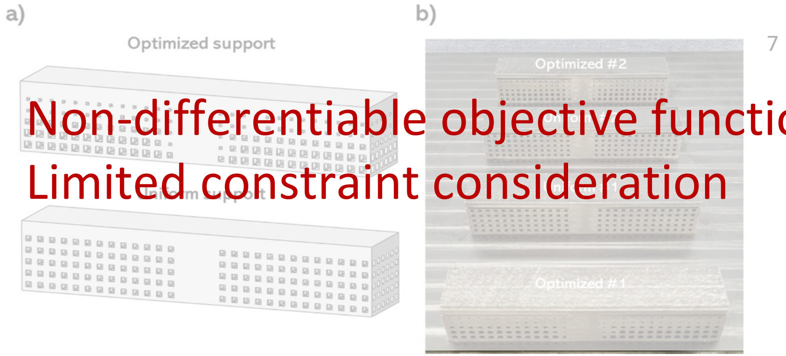

– Non-differentiable objective function

– Limited constraint consideration

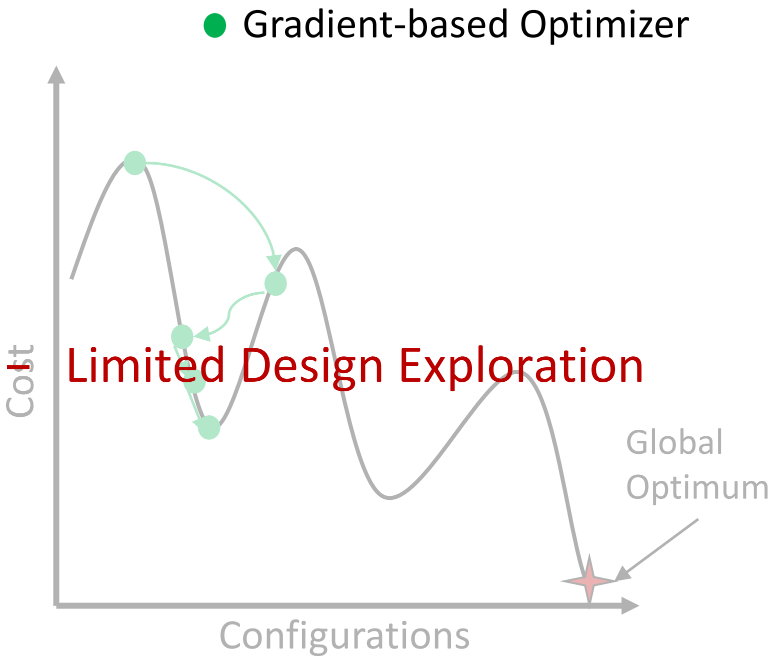

– Limited Design Exploration

4. Jiang, J, et. al (2018) 7. Lee, K.H., et.al (2022) 10. Nazir, A., et. al (2019) 11. Liang, H et. al (2011) 13. Sigmund, O., and Maute, K. (2013) 14. Eberhard, P., et al (1999)

Limitations to Lattice Support Structure Design

Gradient-Based Optimizer[13,14]

✓ Ideal for differentiable objective functions

✓ Fast convergence

– Limited design exploration

Non-Gradient-Based Optimizers[14-16]

✓ Larger design domain exploration

– Computational Expensive

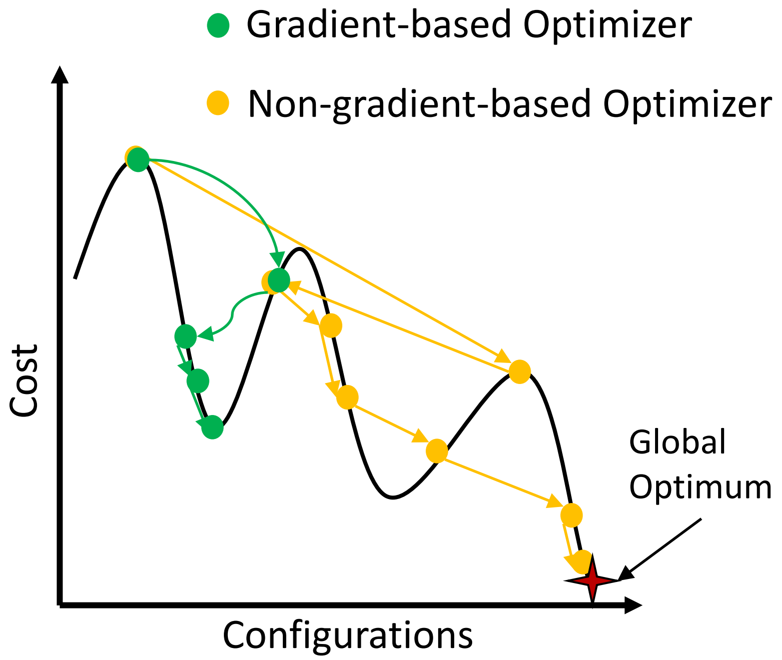

13. Sigmund, O., and Maute, K. (2013) 14. Eberhard, P., et al (1999) 15. Porter, J., et al (2009) 16. Gosselin,L., et al (2009)

1. How can designers *efficiently* find optimally directed lattice support structure solutions that improve heat dissipation while satisfying multiple AM constraints for LPBF?

Lattice Structures for AM

Proposed Lattice Support Structure Methods

– Primarily for horizontal domains

Potential Unit Cells[10]

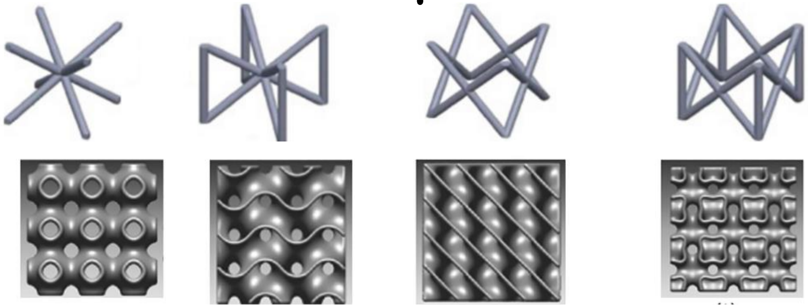

Pin Connection[17,18]:

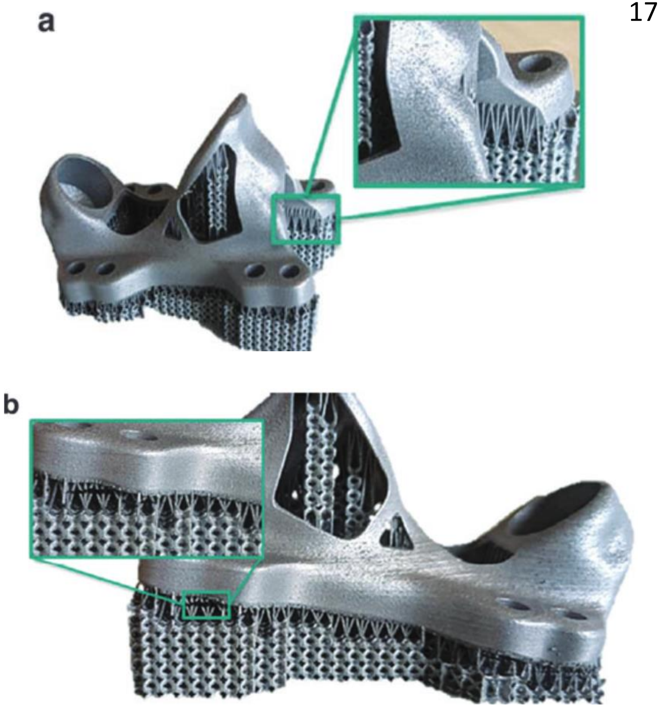

4. Cheng, L., et. al (2019) 9. Huang, R., et. al (2020) 10. Lee, K.H., et.al (2022) 11. Pellens, J., et.al (2020) 12. Hussein, A., et. al (2013) 17. Boos, E., et. al (2022) 18. Bartsch, K., et. al (2020)

1. How can designers *efficiently* find optimally directed lattice support structure solutions that improve heat dissipation while satisfying multiple AM constraints for LPBF?

2. How can lattice support structures be computationally designed to be *attached* to complex structures?

Thesis Statement

To reduce manufacturing and design costs of support structures in laser powder-bed fusion, lattice support structures can be computationally designed to maximize the dissipation of heat while constraining residual stress and deformation for complex structures. By utilizing a modified simulated annealing-based method, designers can efficiently generate optimally directed configurations of pre-defined unit cells with specified functionality at reduced computational costs.

Thesis Statement Breakdown

To reduce manufacturing and design costs of support structures in laser powder-bed fusion, lattice support structures can be computationally designed to maximize the dissipation of heat while constraining residual stress and deformation for complex structures…

Objective 1: A Modified Simulated Annealing Based Method to Design Thermally Conductive Hybrid Lattice Support Structures for LPBF

Thesis Statement Breakdown

To reduce manufacturing and design costs of support structures in laser powder-bed fusion, lattice support structures can be computationally designed to maximize the dissipation of heat while constraining residual stress and deformation for complex structures…

Objective 1: A Modified Simulated Annealing Based Method to Design Thermally Conductive Hybrid Lattice Support Structures for LPBF

Objective 2: An Optimally Directed Lattice Support Structure Design Method for Heat Dissipation and Structural Integrity in LPBF

Thesis Statement Breakdown

To reduce manufacturing and design costs of support structures in laser powder-bed fusion, lattice support structures can be computationally designed to maximize the dissipation of heat while constraining residual stress for complex structures…

Objective 1: A Modified Simulated Annealing Based Method to Design Thermally Conductive Hybrid Lattice Support Structures for LPBF

Objective 2: An Optimally Directed Lattice Support Structure Design Method for Heat Dissipation and Structural Integrity in LPBF

Objective 3: A Multi-Sized Unit Cell Approach to Design Lattice Support Structures for Complex Geometries

Overview

Objective 1: A Modified Simulated Annealing Based Method to Design Thermally Conductive Hybrid Lattice Support Structures for LPBF

- Objective 1.1: Maximize heat dissipation
- Objective 1.2: Introduce expedited evaluation and design exploration

Objective 2: An Optimally Directed Lattice Support Structure Design Method for Heat Dissipation and Structural Integrity in LPBF

- Objective 2.1: Incorporating structural constraints
- Objective 2.2: Expediting thermal and structural property predictions

Objective 3: A Multi-Sized Unit Cell Approach to Design Lattice Support Structures for Complex Geometries

- Objective 3.1: Reduce material waste in transition subdomain
- Objective 3.2: Identify Geometric Representation

Problem Overview

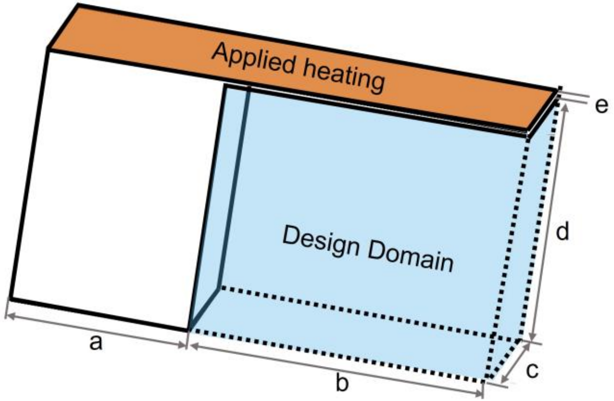

Design Variables (x)

Simple Cubic [4,12,10,19] (SC)

BC Vertical Struts[20,21] (BV)

Face-Centered [9,21,22] (FC)

Find $x = [x_1, x_2, \ldots, x_n]$ to

minimize $Q_{in} = Q(x)$,

subject to $\mathbf{KT} = \mathbf{q}$,

Material Cost → $V(x) < \varepsilon_V * V_{max}$ and

$A(x) < \varepsilon_A * A_{max}$,

4. Cheng, L., et. al (2019) 12. Nazir, A., et. al (2019) 10. Lee, K.H., et.al (2022) 19. Cheng, L., et. al (2018) 20. Vaissier, B., et. al (2019) 21. Downing, D., et. al (2020) 22. Echeta, I., et. al (2020)

Problem Overview

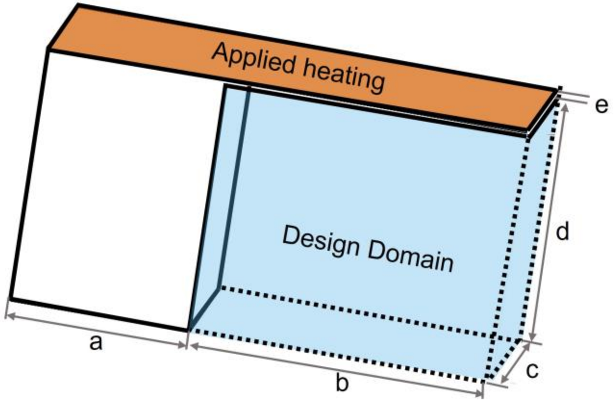

Find $x = [x_1, x_2, \ldots, x_n]$ to

minimize $Q_{in} = Q(x)$,

subject to $\mathbf{KT} = \mathbf{q}$,
$V(x) < \varepsilon_V * V_{max}$ and
$A(x) < \varepsilon_A * A_{max}$,

Design Variables (x)

Simple Cubic [4,12,10,19] (SC)　BC Vertical Struts[20,21] (BV)　Face-Centered [9,21,22] (FC)

Physical properties of the unit cells for AlSi10Mg

Unit Cell	K_{eff} [W/m°C]	Volume [mm^3]	$Area_{XY}$ [mm^2]	$Area_{XZ}$ [mm^2]
Solid	110	8	4	4
SC	12.37	**1.82**	2.31	2.31
BV	24.39	2.82	**0.567**	**1.30**
FC	**39.43**	3.69	0.846	3.24

4. Cheng, L., et. al (2019)　12. Nazir, A., et. al (2019)　10. Lee, K.H., et.al (2022)　19. Cheng, L., et. al (2018)　20. Vaissier, B., et. al (2019)　21. Downing, D., et. al (2020)　22. Echeta, I., et. al (2020)

Defining design domain and boundary conditions

Equivalent Flash Heating Part-Scale[10,23,24]:

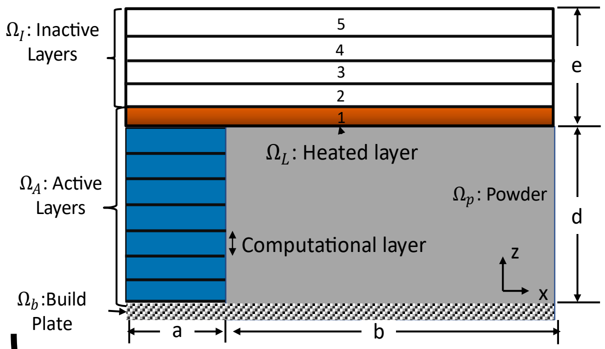

Heating + Cooling

$$\begin{cases} \rho c \dfrac{dT_i(t,x)}{dt} = \nabla \cdot \left(\mathrm{k}\nabla T_i(t,x)\right) + q(\boldsymbol{x}) \\ -\left(\mathrm{k}\nabla T_i(t,x)\right)\cdot n = h\nabla T_i(t,x) \\ T_i(t,\boldsymbol{x}) = T_{base} \\ T = T_{powder} \end{cases}$$

Layer-by-Layer Temperature

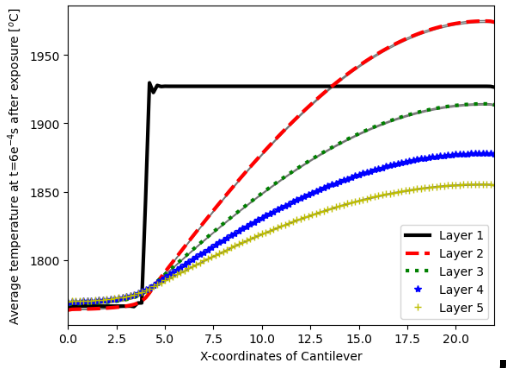

Equivalent steady-state[24]:

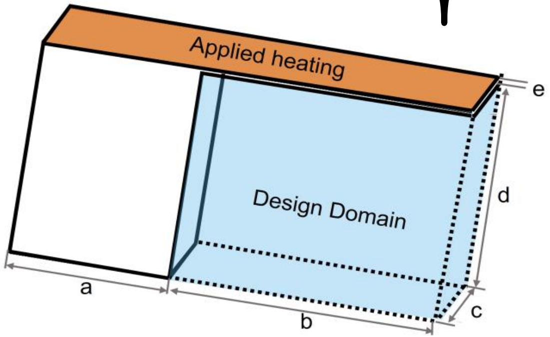

$$\begin{cases} \nabla \cdot (K\nabla \boldsymbol{T}) + \boldsymbol{q} = 0 \\ T(x,y,0) = T_{base} \\ T(x,y,g) = T_{source} \end{cases}$$

10. Lee, K.H., et.al (2022) 23. Li, C., et.al (2017) 24. Subedi, S. C., et.al (2022)

Simulated Annealing (SA)

Analogous to the annealing of metals

Stages:

1. High temperature: **Exploration (1→ 3)**
2. Mid-temperature: **Intermediate (3 → 5)**
3. Low temperature: **Fine-tuning (5 → 6)**

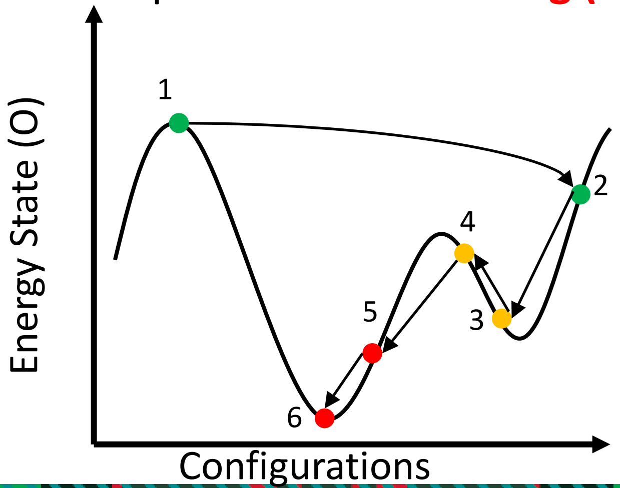

- Annealing Schedule:

$$T_{k+1} = \alpha * T'_k$$

- Probabilistic acceptance of designs:

$$P_{acc} = exp\left(-\frac{O_2 - O_1}{T'_k}\right)$$

Pros:

- Wider exploration of design space
- Allows hill climbing even at later stages (3 → 4)

Cons:

- Computationally expensive

Flowchart of Traditional SA Method

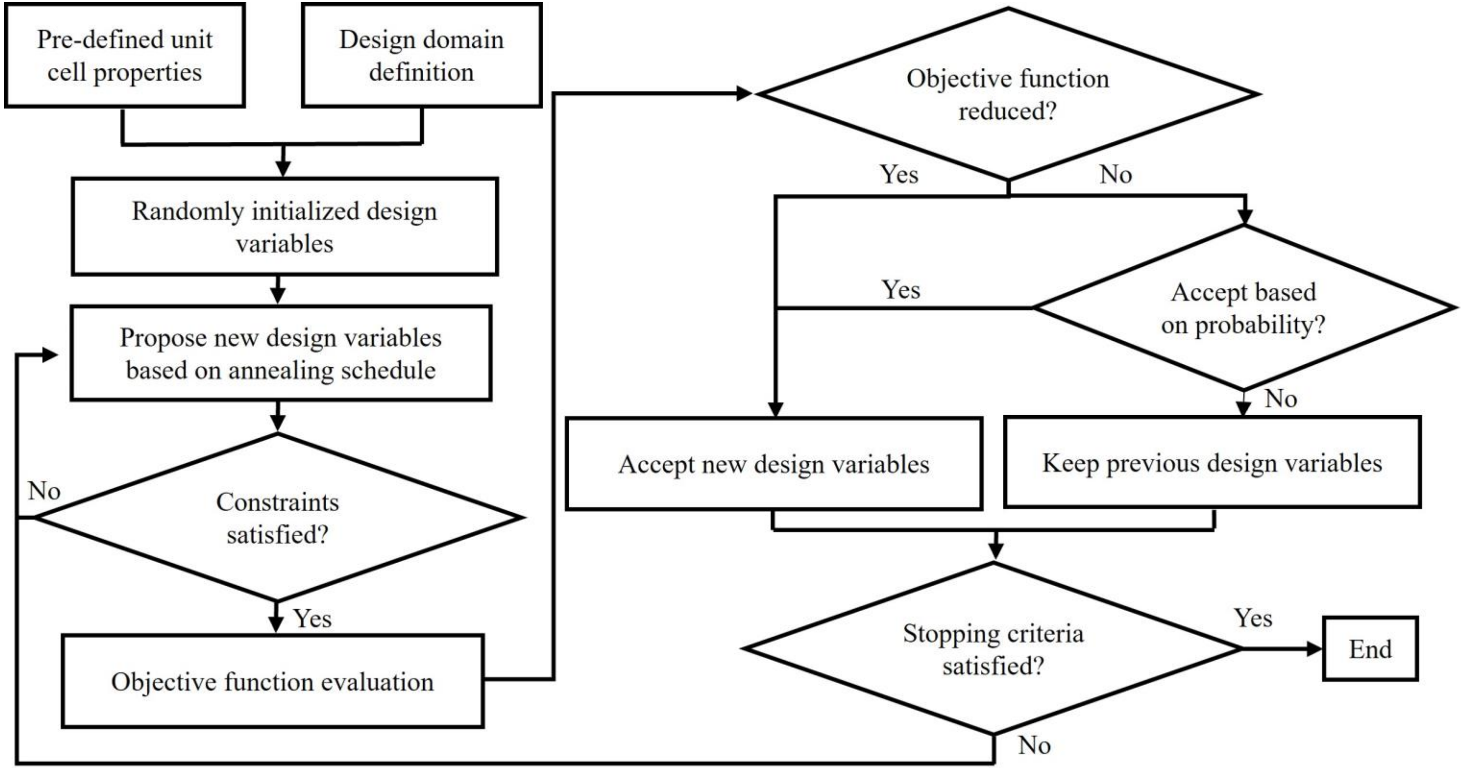

26. Kirkpatrick, S. et. al (1983)

Flowchart of Modified-SA-Based Method

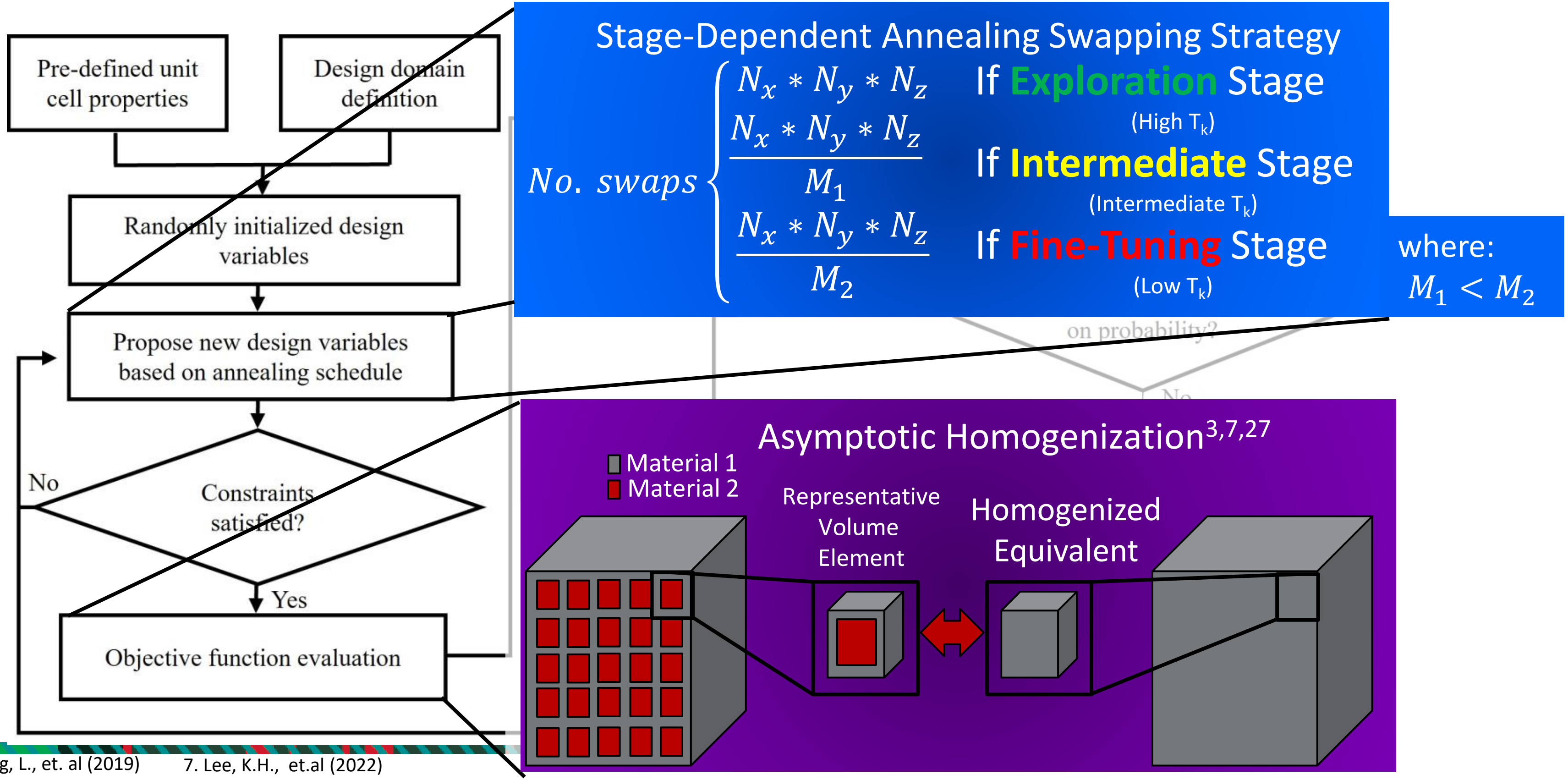

3. Cheng, L., et. al (2019) 7. Lee, K.H., et.al (2022)
27. Hassani, B., and Hinton, E., 1998

Flowchart of Modified-SA-Based Method (M-SAM)

SA Hyperparameters:

T_0=50

α=0.5

Constraints:

V_{max} = 750 mm^3

A_{max} = 140 mm^2

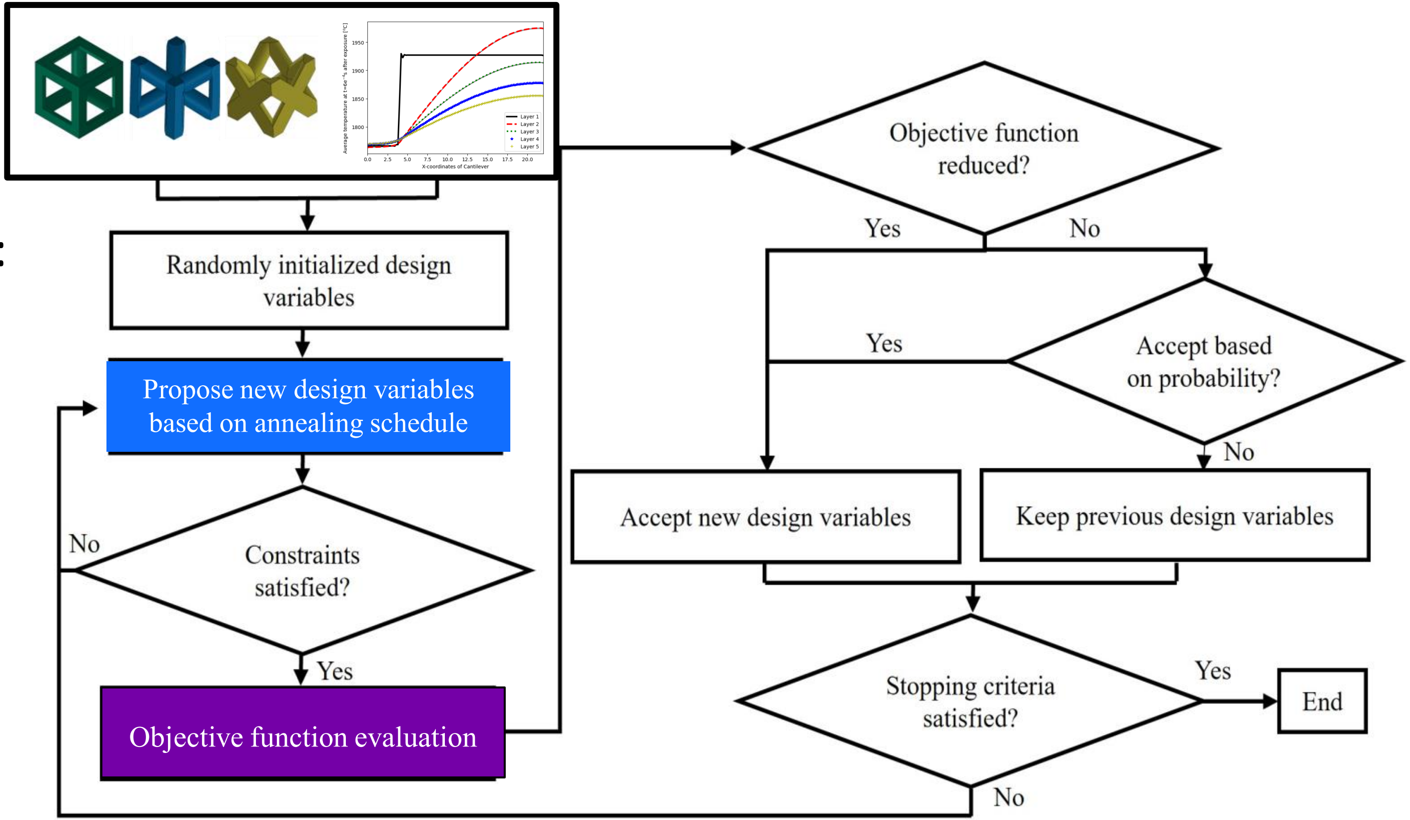

Case Study of Cantilever Beam

Iteration History of 30 runs

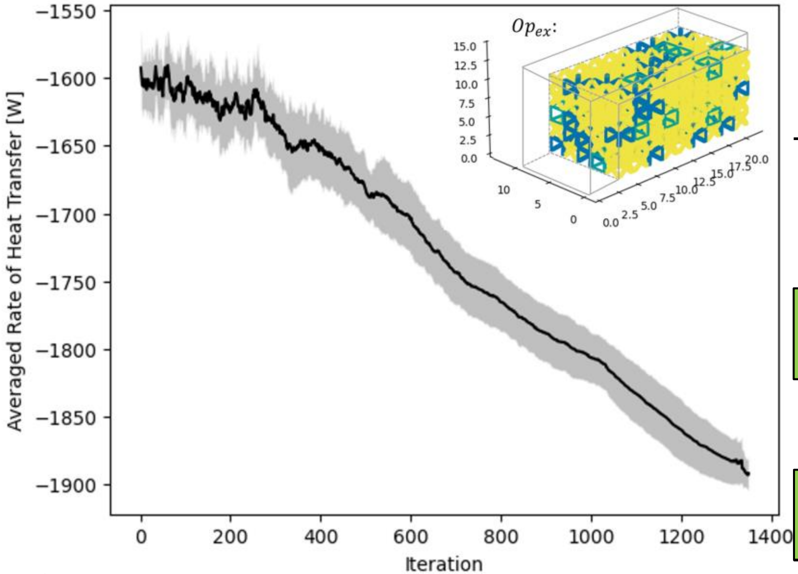

Op_{ex}: Objective = -1,900 W, Volume = 615 mm^3, Area = 106 mm^2.

Comparison of support designs*

	$\lvert Q_{in} \rvert$ [W]	Volume V(x) [mm^3]	Area A(x) [mm^2]	SC/BV/FC	Constraint Satisfaction V(x) < 750 A(x) < 140
Solid	4,546	1,800	280	0/0/0	No
SC Only	1,196	409	161	225/0/0	No
BV Only	1,607	**634**	57	0/225/0	Yes
FC Only	2,124	830	120	0/0/225	No
Op_{Avg}	**1,887 (15.0)**	745 (5.56)	**108 (4.94)**	**18/58/149 (3.23/5.43/5.34)**	**Yes**

*standard deviation in ( )

Compared to BV Only — Average of ~16% Heat dissipation

Overview

Objective 1: A Modified Simulated Annealing Based Method to Design Thermally Conductive Hybrid Lattice Support Structures for LPBF

- Objective 1.1: Maximize heat dissipation
- Objective 1.2: Introduce expedited evaluation and design exploration

Objective 2: An Optimally Directed Lattice Support Structure Design Method for Heat Dissipation and Structural Integrity in LPBF

- Objective 2.1: Incorporating structural constraints
- Objective 2.2: Expediting thermal and structural property predictions

Objective 3: A Multi-Sized Unit Cell Approach to Design Lattice Support Structures for Complex Geometries

- Objective 3.1: Reduce material waste in transition subdomain
- Objective 3.2: Automating Unit Cell Placement

Definition of Model

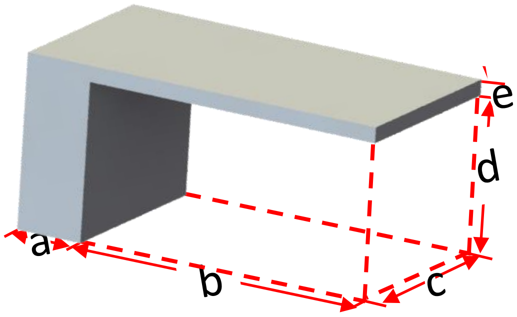

Example: Cantilever Beam

Design Variables (x)

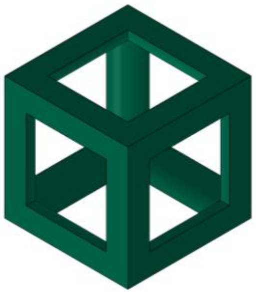

Simple Cubic [4,12,10,19]
(SC)

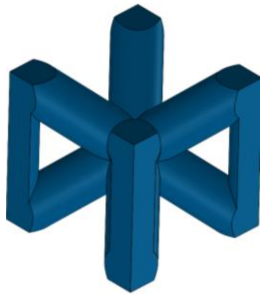

BC Vertical Struts[20,21]
(BV)

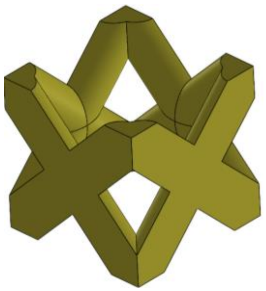

Face-Centered [9,21,22]
(FC)

Find $x = [x_1, x_2, \ldots, x_n]$ to

minimize $Q_{in} = Q(x)$,

subject to
KT = **q**,
CU = F, ← Static-Structural
$V(x) < \varepsilon_V * V_{max}$ and
$A(x) < \varepsilon_A * A_{max}$,
$\frac{\sigma_j^{PN}}{\sigma_y}_{max} \leq 1$
$U_{tot} \leq U_{max}$

Physical properties of the unit cells for AlSi10Mg

Unit Cell	$K_{eff}\left[\frac{W}{mC}\right]$	$Volume\ [mm^3]$	$Area_{XY}\ [mm^2]$	$Area_{YZ}\ [mm^2]$	E_{eff_Z} $[Pa]$	$E_{eff_{Y,X}}$ $[Pa]$	G_{xy} [Pa]	G_{xz}/G_{yz} [Pa]
Solid	110	8	4	4	7.4E+10	7.4E+10	2.782E+10	2.782E+10
SC	12.37	**1.82**	2.31	2.31	7.64E+09	7.64E+09	5.419E+08	5.419E+08
BV	24.39	2.82	**0.567**	**1.30**	9.73E+09	3.69E+09	**4.375E+09**	4.175E+09
FC	**39.43**	3.69	0.846	3.24	**1.95E+10**	**1.34E+10**	1.598E+08	**6.873E+09**

Structural Constraints

P-Norm Stress[4,28]:

$$\sigma_j^{PN}(x) = \left(\frac{1}{N_j}\sum_{a\in\Omega_j}\left(\sigma_a^{vM}(x)\right)^p\right)^{\frac{1}{p}}$$

$\sigma_j^{PN} > \sigma_y$:= plastic deformation

$\sigma_j^{PN} < \sigma_y$:= elastic deformation

Maximum Total Displacement: $U_{tot} = \sqrt{U_x^2 + U_y^2 + U_z^2}$

Recoater Collision[11,29,30]

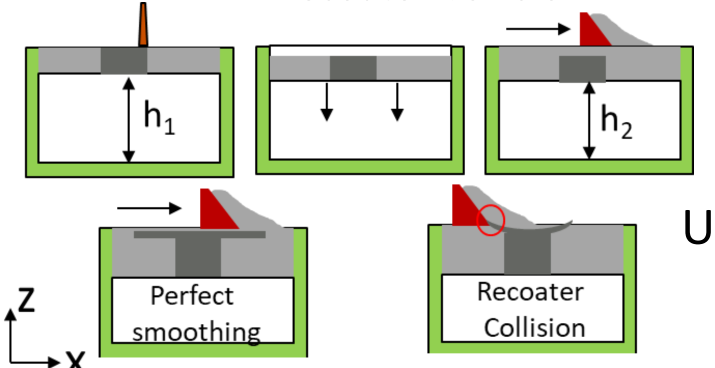

$U_z \leq h_1 - h_2$

$U_z > h_1 - h_2$

$U_z = L/\rho_{shr}$

Draft Angle (γ)[31]

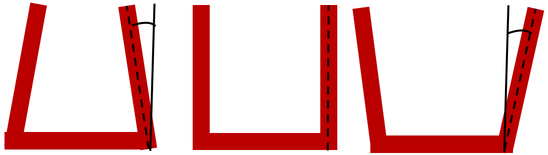

$\gamma < 0$ $\gamma = 0$ $\gamma > 0$

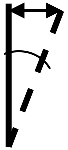

$U_x = U_y$

4. Cheng, L., et. al (2019) 11. Pellens, J., et.al (2020) 28. Holmberg, E., et. al (2013) 29. Zhang, Z. D,. et. al (2020) 30. Misiun, G., et. al (2013) 31. Sulaiman, S., et. al (2013)

Defining design domain and boundary conditions

Part Scale Modeling

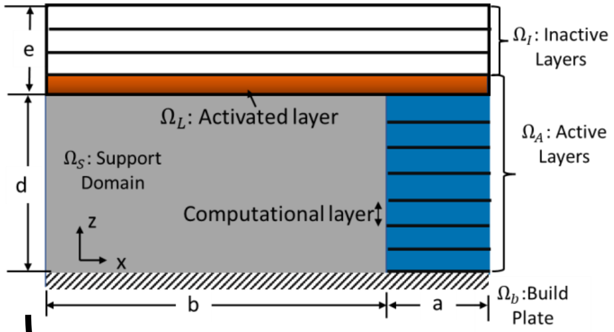

1. Inherent Strain Method (ISM) [4,11,29,30,32,33]

$$
\begin{cases}
\nabla \cdot \sigma_i = 0 \\
\sigma_i = \mathbf{C}\varepsilon_e^i \\
\varepsilon_{tot}^i = \varepsilon_e^i + \varepsilon_p^i + \varepsilon_{in}^i,
\end{cases}
$$

+

2. Equivalent Flash Heating (EFH) [10,23,24]

Heating + Cooling

$$
\begin{cases}
\rho c \dfrac{dT_i(t,x)}{dt} = \nabla \cdot \left(\mathrm{k}\nabla T_i(t,x)\right) + q(\boldsymbol{x}) \\
-\left(\mathrm{k}\nabla T_i(t,x)\right) \cdot n = h\nabla T_i(t,x) \\
T_i(t,\boldsymbol{x}) = T_{base} \\
T = T_{powder}
\end{cases}
$$

Equivalent Steady-State

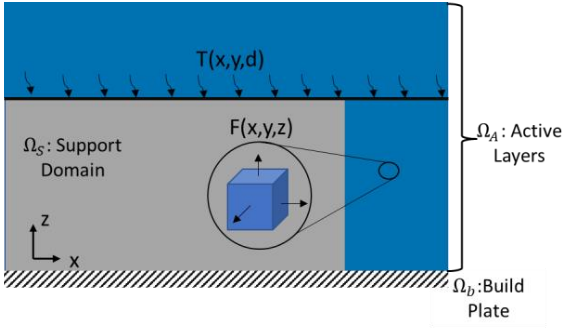

Static Structural [29]

$$
\begin{cases}
\nabla \cdot \sigma + \boldsymbol{F} = 0 \\
U(x,y,0) = 0
\end{cases}
$$

+

Steady-State Thermal [24]

$$
\begin{cases}
\nabla \cdot (K\nabla \boldsymbol{T}) + \boldsymbol{q} = 0 \\
T(x,y,0) = T_{base} \\
T(x,y,d) = T_{source}
\end{cases}
$$

4. Cheng, L., et. al (2019) 11. Pellens, J., et.al (2020) 24. Subedi, S. C., et.al (2022) 29. Zhang, Z. D,. et. al (2020) 30. Misiun, G., et. al (2013) 32. Liang, X., et. al (2018) 33. Chen, Q., et. al (2019)

Flowchart of Modified SA-based Method (M-SAM)

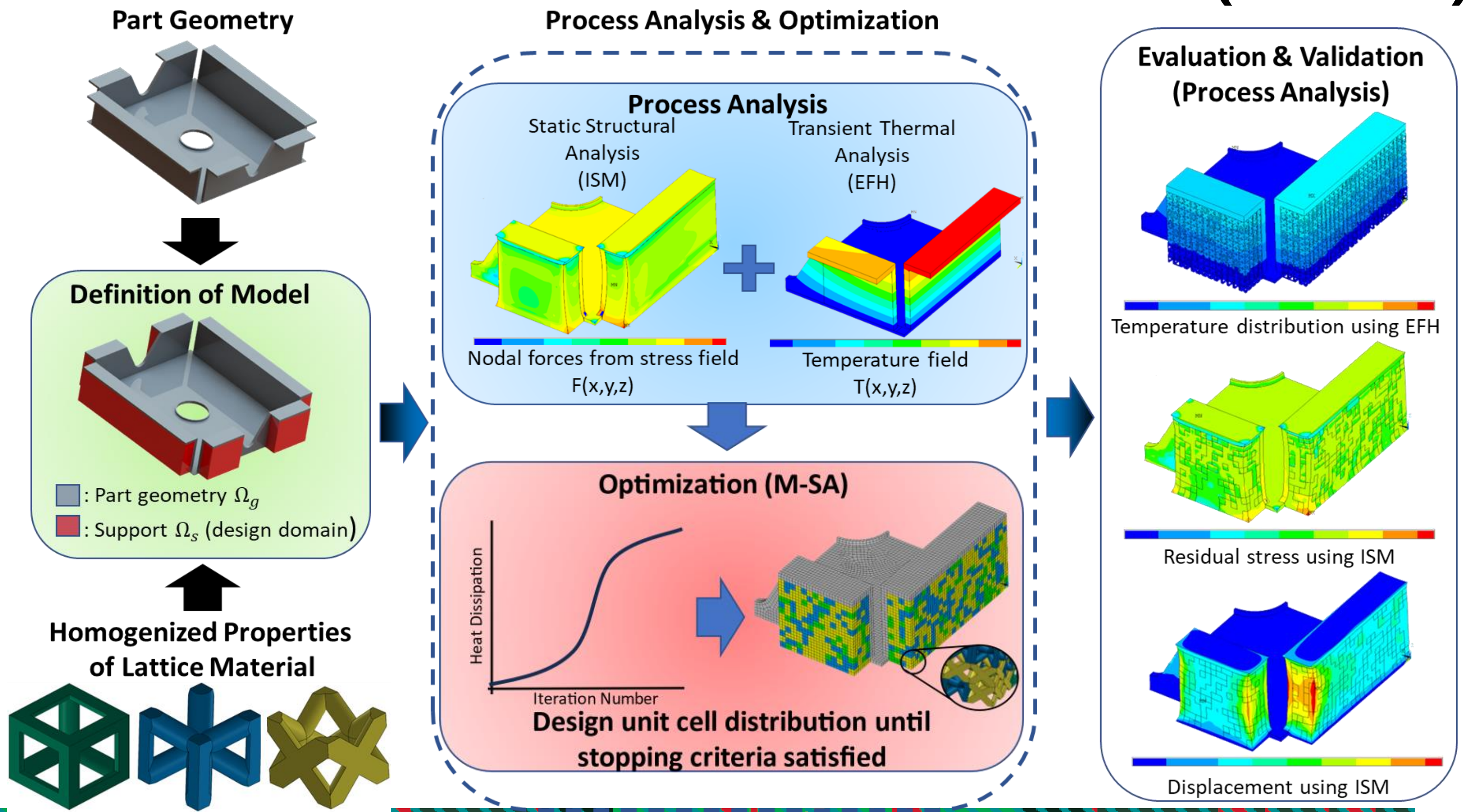

Case Study of Cantilever Beam

Iteration History of 30 runs

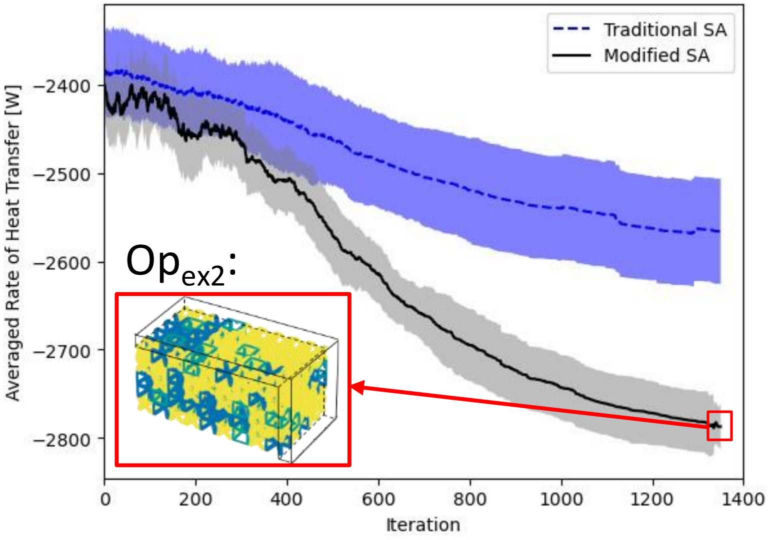

Objective = -2,815 W, Volume = 735 mm^3, Area = 108 mm^2, p-Norm = 0.366, U_{sum} = 24.2 mm

Comparison of support designs*

	$\lvert Q_{in} \rvert$	V(x)	A(x)	P-norm Stress	Max(U_{sum}) [μm]	SC/BV/FC	V(x)<750 A(x)<140 P-norm < 0.66 Max(U_{sum}) < 32
Solid	7,128	1,800	280	0.293	8.06	--	No
SC Only	1,743	409	161	0.359	31.7	225/0/0	No
BV Only	2,405	**634**	**57**	0.365	30.8	0/225/0	Yes
FC Only	3,235	830	120	0.352	15.6	0/0/225	No
$Op_{avg,2}$	**2,773 (47.1)**	722 (11.7)	107 (6.82)	**0.360 (0.00614)**	**24.0 (1.34)**	**27/63/133 (5.3/8.0/9.4)**	Yes

*standard deviation in ( )

Compared to BV Only

Average of ~14% Heat dissipation

Average of ~25% Distortion

Case Study of Aerospace Bracket

Iteration History of 30 runs

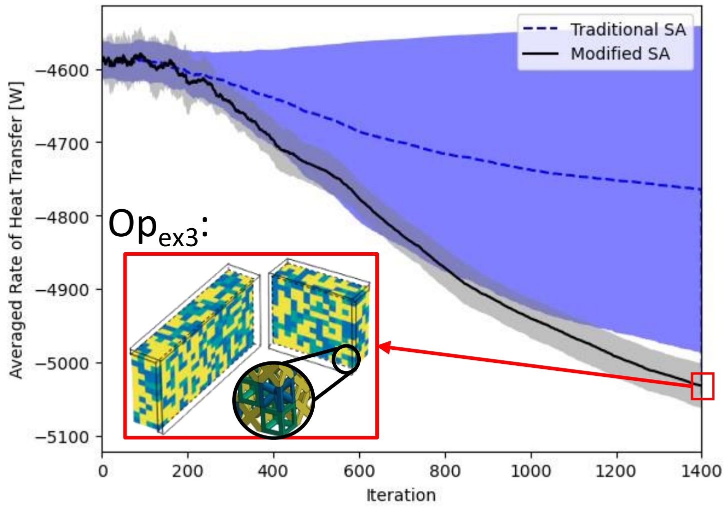

Objective = -5,039 W, Volume = 5,481 mm^3, Area = 1,243 mm^2, p-Norm = 0.648, U_{sum} = 69.7 mm

Comparison of support designs*

	$\lvert Q_{in} \rvert$	V(x)	A(x)	P-norm Stress	$Max(U_{sum})$ [μm]	SC/BV/FC	V(x) < 5,900 A(x) < 1,360 P-norm < 0.66 $Max(U_{sum})$< 76
Solid	12,479	14,208	2,368	0.609	14	--	No
SC Only	3,524	3,232	1,367	0.648	96.0	1,776/0/0	No
BV Only	4,624	5,008	[illegible]	0.648	97.5	0/1,776/0	No
FC Only	6,004	6,553	1,568	0.637	74.7	0/0/1,776	No
$Op_{avg,3}$	**4,902 (29.4)**	**5,315 (36.2)**	**1,222 (13.7)**	**0.643 (0.0037)**	**72.8 (2.3)**	**388/589/799 (16/20/30)**	**Yes**

Satisfies Constraints

Average of ~60% Material Cost

Average of ~47% Post-processing Cost

*standard deviation in ( )

34. Xiaohui, J., et. al (2022)

Overview

Objective 1: A Modified Simulated Annealing Based Method to Design Thermally Conductive Hybrid Lattice Support Structures for LPBF

- Objective 1.1: Maximize heat dissipation
- Objective 1.2: Introduce expedited evaluation and design exploration

Objective 2: An Optimally Directed Lattice Support Structure Design Method for Heat Dissipation and Structural Integrity in LPBF

- Objective 2.1: Incorporating structural constraints
- Objective 2.2: Expediting thermal and structural property predictions

Objective 3: A Multi-Sized Unit Cell Approach to Design Lattice Support Structures for Complex Geometries

- Objective 3.1: Reduce material waste in transition subdomain
- Objective 3.2: Automating Unit Cell Placement

Reducing Material Waste using Multi-Sized Unit Cells

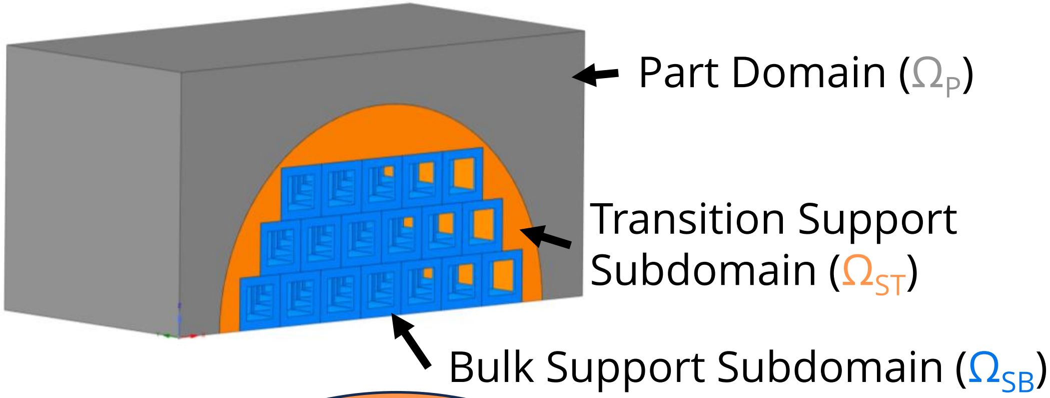

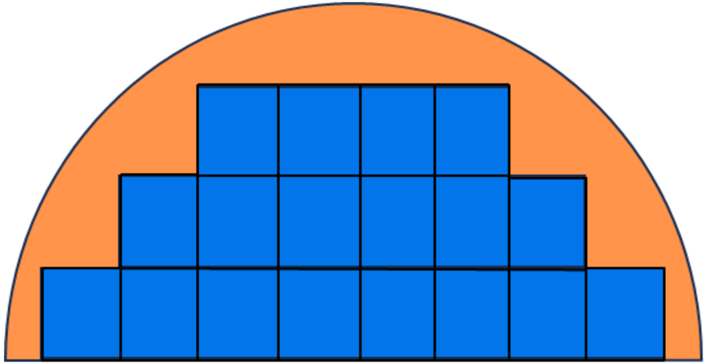

Single Sized Unit Cells

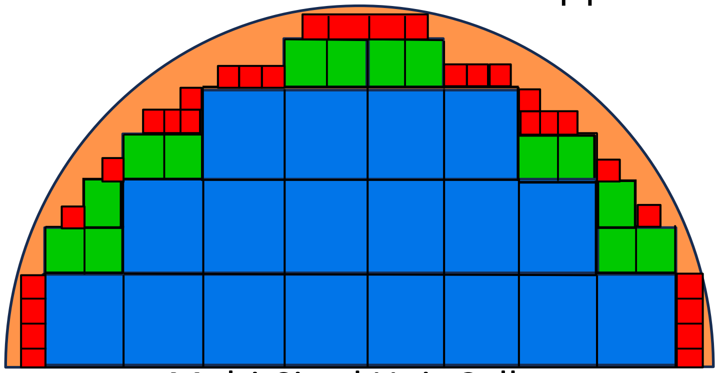

Multi-Sized Unit Cells

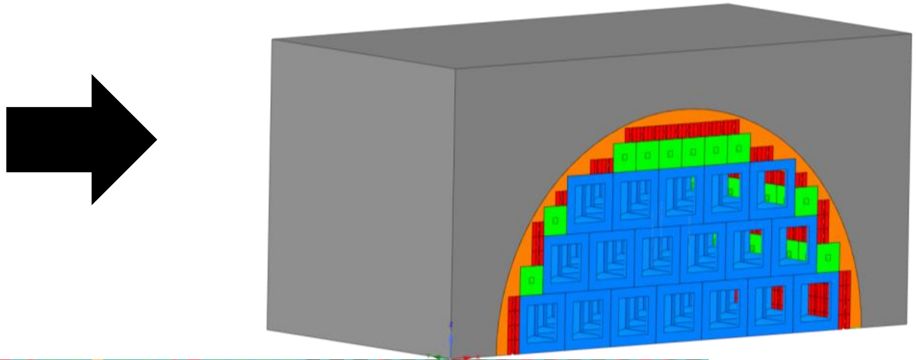

Definition of Model

Example: Symmetric Curved Pipe

Find $x = [x_1, x_2, \ldots, x_n]$ and $y = [y_1, y_2, \ldots, y_m]$ to

minimize $Q_{in} = Q(x)$,

subject to
$\mathbf{KT} = \mathbf{q}$,
$\mathbf{CU} = \mathbf{F}$,
$\frac{\sigma_j^{PN}}{\sigma_y} \leq \sigma_{max}$,
$U_z \leq U_{max}$, and
$V(x) < V_{max}$

Design Variables (x)

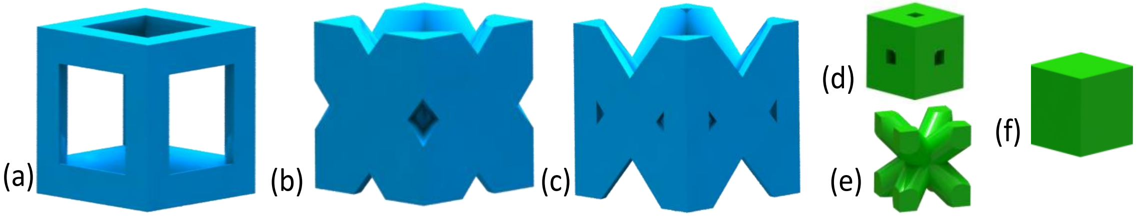

Physical properties of the unit cells for Haynes 282

Size	Unit Cell	$K_{eff,z}\left[\frac{W}{mC}\right]$	E_{eff_z} $[GPa]$	G_{xy} $[GPa]$	G_{xz}/G_{yz} $[GPa]$	$Volume$ $[mm^3]$
2 mm	(a) SC	1.54	30.8	2.92	2.92	**1.82**
	(b) FC	**5.58**	**79.5**	**14.6**	**32.6**	3.69
	(c) TR	2.96	31.3	2.07	1.39	3.02
1 mm	(d) sc	6.84	135	44.8	44.8	0.7839
	(e) bc[21,22,35]	3.79	39.4	26.7	26.7	**0.5571**
	(f) sol	**10.30**	**217**	**82.2**	**82.2**	1

21. Downing, D., et. al (2020) 22. Echeta, I., et. al (2020) 35. Dong, G., et. al (2017)

Voxel-Mesh Based Multi-Sized Unit Cell Approach

Input

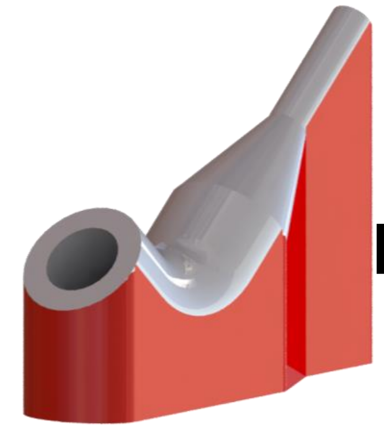

Part Domain
+
Support Domains

Voxelization

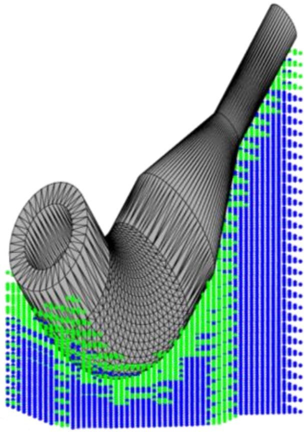

- Convert to voxel[36]
- Identify support domain
- Sort voxels based on unit size

Output

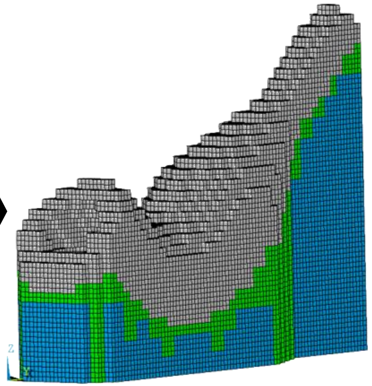

Voxel Mesh

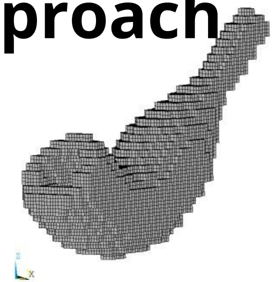

Part Domain + Transition Subdomains

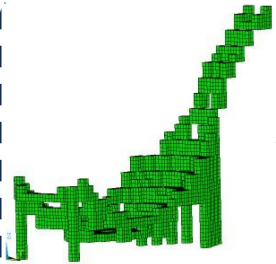

Size 1

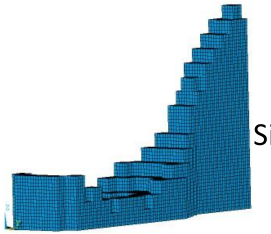

Size 2

Bulk Support Subdomain

36. Aitkenhead, A. (2013)

Flow Chart of Modified M-SAM

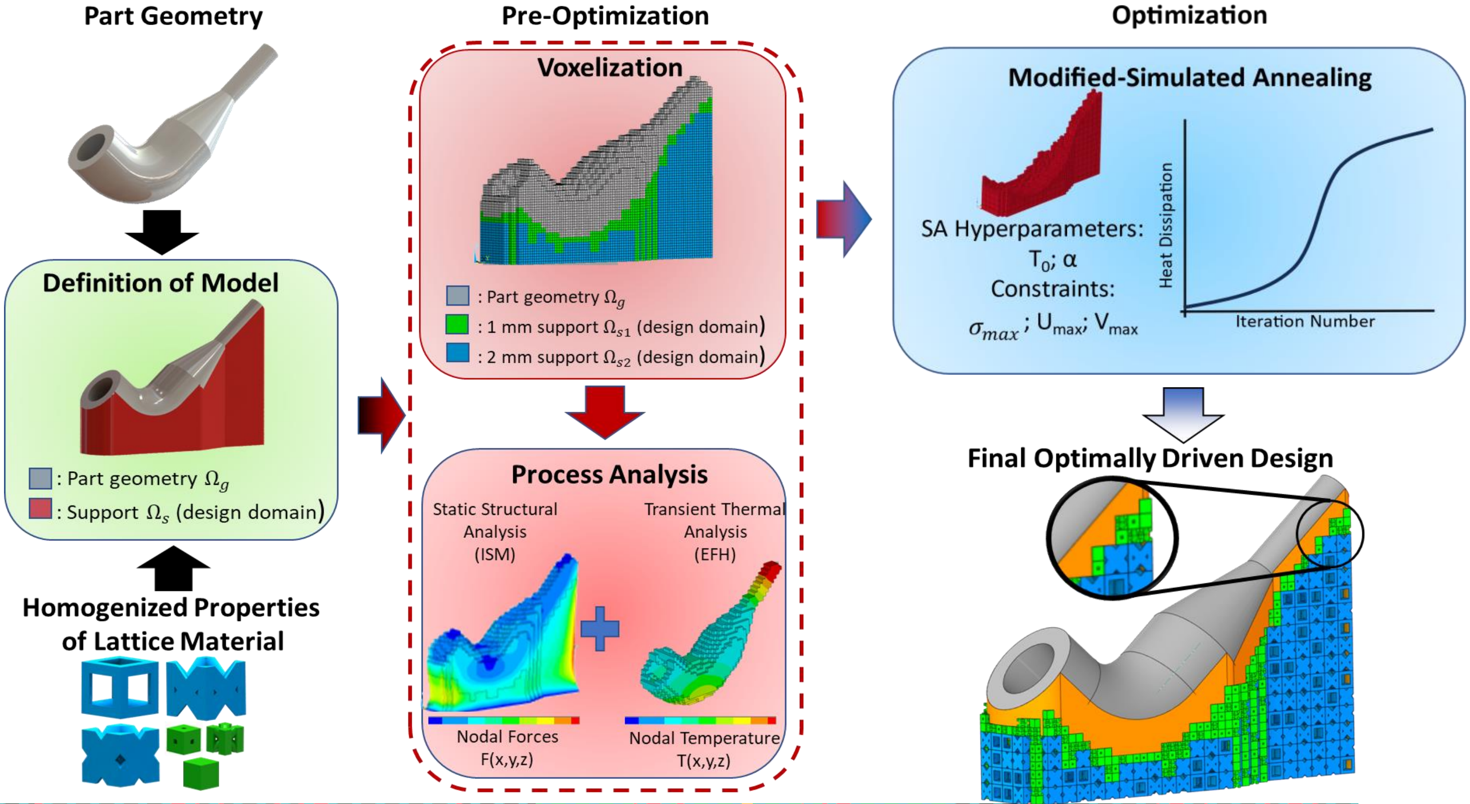

Case Study of Heat Exchanger Adapters

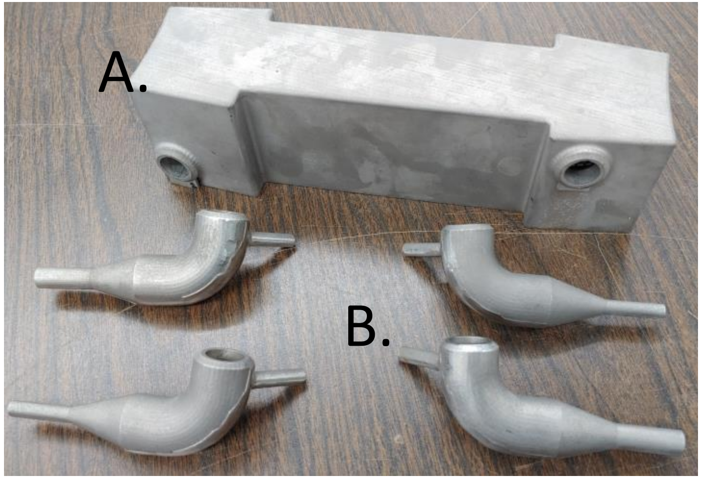

A. sCO_2 heat exchanger

B. Heat Exchanger Adapters

Failed Prints

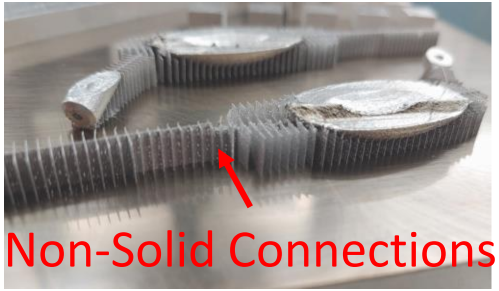

Successful Prints

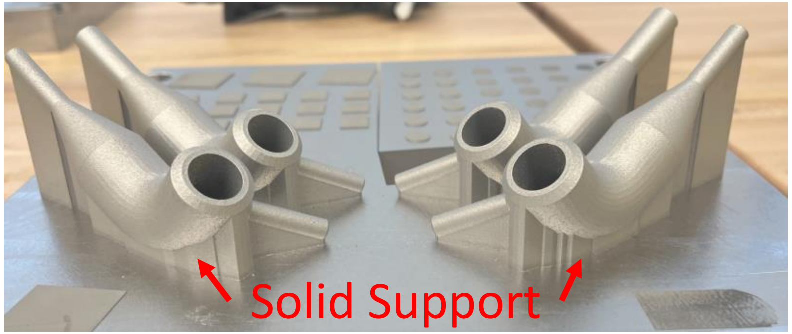

37. Krol, T.A., et. al (2012)

Collaborators: Prof. Tony Rollett, Junwon Seo and Nicholas Lamprinakos

Case Study of Heat Exchanger Adapter

Iteration History of 30 runs

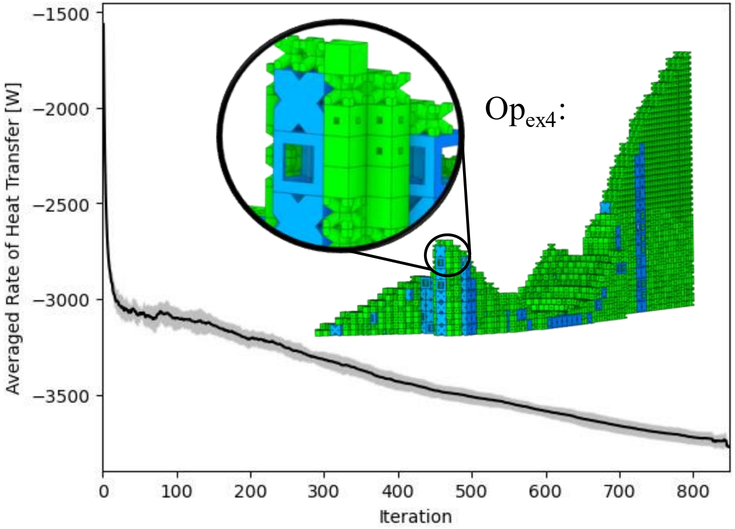

Objective = -3,742 W, Volume = 3,807mm^3, p-Norm = 0.08, U_{sum} = 18.24 mm

Comparison of support designs*

	$\lvert Q_{in} \rvert$	V(x)	P-norm Stress	Max(U_z) [μm]	SC/TR/FC sc/bv/sol	V(x) < 3,808 P-norm < 0.66 Max(U_z)< 40
Solid	6,470	7,617	0.053	4.6	--	No
SC Only	3,182	**3,711**	0.166	19.45	631/0/0 0/0/2,563	Yes
TR Only	3,756	4,468	0.108	13.07	0/631/0 0/0/2,563	No
FC Only	4,775	4,891	0.072	8.08	0/0/1,776 0/0/2,563	No
Op$_{avg,4}$	**3,742 (38)**	3,802 (8.8)	**0.087 (0.004)**	**16.0 (0.51)**	**151/185/295 645/1,228/689 (6/12/11/18/16/21)**	**Yes**

*standard deviation in ( )

Compared to SC Only ↑ Average of ~16% Heat Dissipation ↓ Average of ~19% Distortion

Summary

Question 1: How can designers *efficiently* find optimally directed lattice support structure solutions that improve heat dissipation while satisfying multiple AM constraints for LPBF?

Objective 1: A Modified Simulated Annealing Based Method to Design Thermally Conductive Hybrid Lattice Support Structures for LPBF

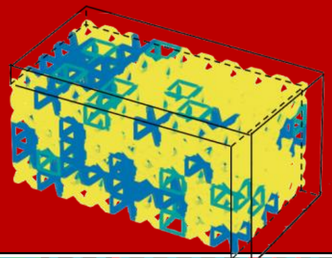

Objective 2: An Optimally Directed Lattice Support Structure Design Method for Heat Dissipation and Structural Integrity in LPBF

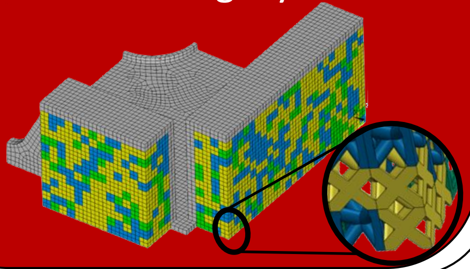

Question 2: How can lattice support structures be computationally designed to be *attached* to complex structures?

Objective 3: A Multi-Sized Unit Cell Approach to Design Lattice Support Structures for Complex Geometries

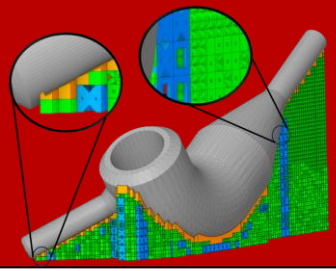

Contributions

1. Introducing a method to **increase efficiency** of non-gradient-based optimizers with reduced computational costs

2. Establishing a method to incorporate both **thermal and structural** simulation-informed evaluations for lattice support structures

3. Developing an approach to broaden the application of lattice support structure to **complex geometries**

Objective 1

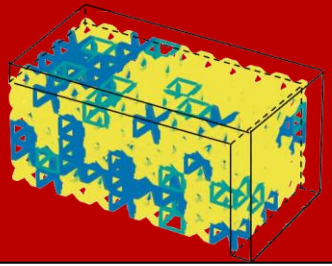

Objective 2

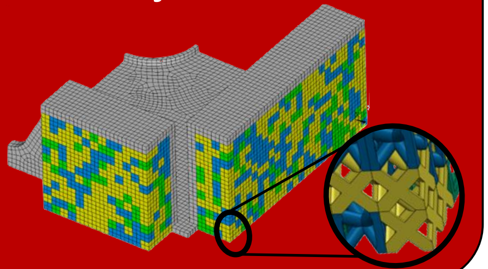

Objective 3

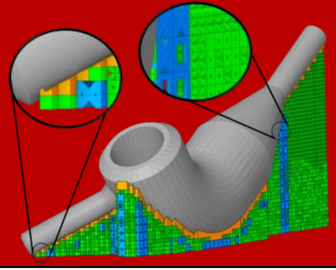

Future Work

Physical Structure Validation

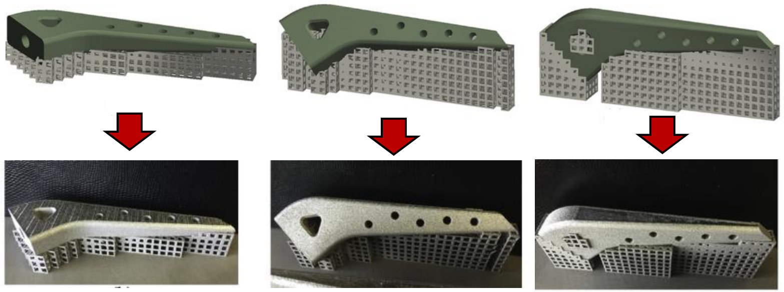

3

Evaluating Lattice Printability

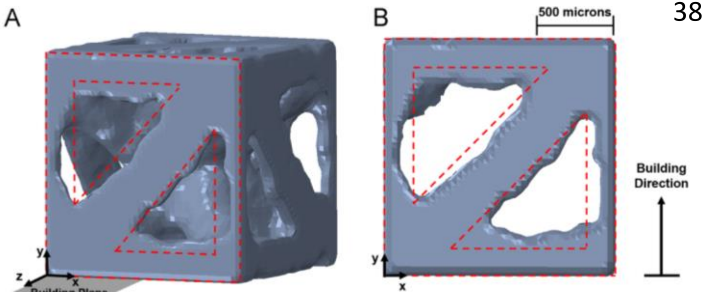

38

Guidelines for choosing pre-defined unit cells

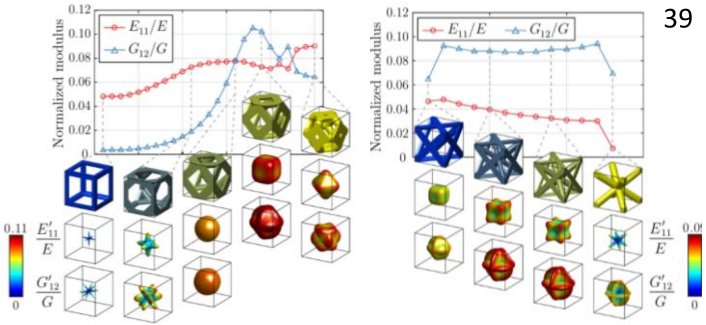

39

Parameterizing Transition Subdomain

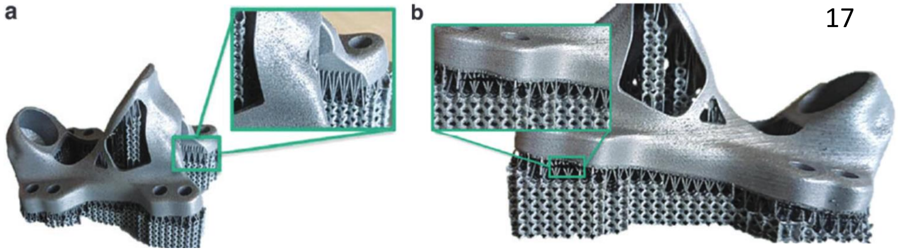

17

3. Cheng, L., et. al (2019) 17. Boos, E., et. al (2022) 38. Bagheri, Z., et. al (2016) 39. Sanders, E., et. al (2021)

Acknowledgements

Supported by:

GEM
THE NATIONAL GEM CONSORTIUM

ARL

Integrated Design Innovation Group

Carnegie Mellon University
Computational Bio-Modeling Lab

Committee:


Prof. Cagan

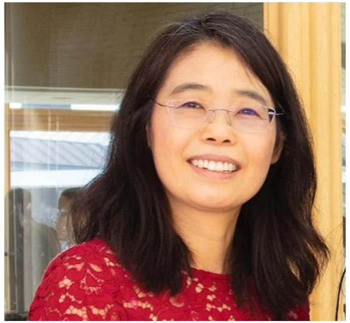
Prof. Zhang


Prof. Rollett


Dr. Zhang

Acknowledgements

Thank you

Questions?

References

Conference Papers

1. **White, L.**, Liang, X., Zhang, G., Cagan, J., and Zhang, Y. J. "Coupling Simulated Annealing and Homogenization to Design Thermally Conductive Hybrid Lattice Support Structures for LPBF". Accepted in Proceedings of the ASME 2024 International Design Engineering Technical Conferences & Computers and Information in Engineering Conference, Boston, Massachusetts, 2023.
2. X. Liang, **L. White**, J. Cagan, A. D. Rollett, Y. J. Zhang. Design and Printability Evaluation of Heat Exchangers for Laser Powder Bed Fusion Process. ASME International Design Engineering Technical Conference & Computers and Information in Engineering Conference (IDETC/CIE). St. Louis, MI. Aug 14-17, 2022.

Journal Papers

1. **White, L.**, Liang, X., Zhang, G., Cagan, J., and Zhang, Y. J. "A Modified Simulated Annealing-Based Method for Hybrid Lattice Support Structure Design in LPBF Additive Manufacturing". *Under review for Journal of Computing and Information Science in Engineering*, 2023.
2. X. Liang, **L. White**, J. Cagan, A. D. Rollett, Y. J. Zhang. "Unit-Based Design of Cross-Flow Heat Exchangers for LPBF". *Journal of Mechanical Design*. 2023

References

[1] Vafadar, A., Guzzomi, F., Rassau, A., and Hayward, K., 2021, “Advances in Metal Additive Manufacturing A Review of Common Processes, Industrial Applications, and Current Challenges,” Applied ciences, **11**(3), p. 1213.

[2] Wang, D., Wei, X., Liu, J., Xiao, Y., Yang, Y., Liu, L., Tan, C., Yang, X., and Han, C., 2022, “Lightweight Design of an AlSi10Mg Aviation Control Stick Additively Manufactured by Laser Powder Bed Fusion,” Rapid Prototyping Journal, **28**(10), pp. 1869–1881.

[3] Li, C., Liu, Z. Y., Fang, X. Y., and Guo, Y. B., 2018, “Residual Stress in Metal Additive Manufacturing,” Procedia CIRP, **71**, pp. 348–353.

[4] Cheng, L., Liang, X., Bai, J., Chen, Q., Lemon, J., and To, A., 2019, “On Utilizing Topology Optimization to Design Support Structure to Prevent Residual Stress Induced Build Failure in Laser Powder Bed Metal Additive Manufacturing,” Additive Manufacturing, **27**, pp. 290–304.

[5] Jiang, J., Xu, X., and Stringer, J., 2018, “Support Structures for Additive Manufacturing: A Review,” JMMP, **2**(4), p. 64.

[6] Bartsch, K., Herzog, D., Emmelmann, C., and Lange, F., 2019, “A Novel Approach to Support Structures Optimized for Heat Dissipation in SLM by Combining Process Simulation with Topology Optimization,” The NAFEMS World Congress Quebec City, Quebec, QC, Canada.

[7] Bartsch, K., Herzog, D., Emmelmann, C., and Lange, F., 2019, “A Novel Approach to Support Structures Optimized for Heat Dissipation in SLM by Combining Process Simulation with Topology Optimization,” The NAFEMS World Congress Quebec City, Quebec, QC, Canada.

[8] Miki, T., and Nishiwaki, S., 2022, “Topology Optimization of the Support Structure for Heat Dissipation in Additive Manufacturing,” Finite Elements in Analysis and Design, **203**, p. 103708.

[9] Huang, R., Dai, N., Cheng, X., and Wang, L., 2020, “Topology Optimization of Lattice Support Structures for Heat Conduction in Selective Laser Melting,” Int J Adv Manuf Technol, **109**(7–8), pp. 1841–1851.

[10] Lee, K.-Hyun., and Yun, G. J., 2022, “Design Optimization of Thermally Conductive Support Structure for Laser Powder-Bed Fusion Process with Part-Scale Thermal History,” Additive Manufacturing, **51**, p. 102627.

[11] Pellens, J., Lombaert, G., Michiels, M., Craeghs, T., and Schevenels, M., 2020, “Topology Optimization of Support Structure Layout in Metal-Based Additive Manufacturing Accounting for Thermal Deformations,” Struct Multidisc Optim, **61**(6), pp. 2291–2303.

[12] Nazir, A., Abate, K. M., Kumar, A., and Jeng, J.-Y., 2019, “A State-of-the-Art Review on Types, Design, Optimization, and Additive Manufacturing of Cellular Structures,” Int J Adv Manuf Technol, **104**(9), pp. 3489–3510.

[13] Liang, H., Raymont, D., Chunze, Y., Hussein, A., and Young, P., eds., 2011, *Design and Additive Manufacturing of Cellular Lattice Structures*, CRC Press.

References

[14] Hassani, B., and Hinton, E., 1998, “A Review of Homogenization and Topology Optimization I—Homogenization Theory for Media with Periodic Structure,” Computers & Structures, **69**(6), pp. 707–717.

[15] Sigmund, O., and Maute, K., 2013, “Topology Optimization Approaches,” Struct Multidisc Optim, **48**(6), pp. 1031–1055.

[16] Eberhard, P., Schiehlen, W., and Bestle, D., 1999, “Some Advantages of Stochastic Methods in Multicriteria Optimization of Multibody Systems,” Archive of Applied Mechanics, **69**(8), pp. 543–554.

[17] Porter, J. M., Larsen, M. E., and Howell, J. R., 2009, “Discrete Optimization of Radiant Heaters with Simulated Annealing,” American Society of Mechanical Engineers Digital Collection, pp. 903–908.

[18] Gosselin, L., Tye-Gingras, M., and Mathieu-Potvin, F., 2009, “Review of Utilization of Genetic Algorithms in Heat Transfer Problems,” International Journal of Heat and Mass Transfer, **52**(9), pp. 2169–2188.

[19] Cheng, L., Liu, J., Liang, X., and To, A. C., 2018, “Coupling Lattice Structure Topology Optimization with Design-Dependent Feature Evolution for Additive Manufactured Heat Conduction Design,” Computer Methods in Applied Mechanics and Engineering, **332**, pp. 408–439

[20] Vaissier, B., Pernot, J.-P., Chougrani, L., and Véron, P., 2019, “Genetic-Algorithm Based Framework for Lattice Support Structure Optimization in Additive Manufacturing,” Computer-Aided Design, **110**, pp. 11–23.

[21] Downing, D., Leary, M., McMillan, M., Alghamdi, A., and Brandt, M., 2020, “Heat Transfer in Lattice Structures during Metal Additive Manufacturing: Numerical Exploration of Temperature Field Evolution,” RPJ, **26**(5), pp. 911–928.

[22] Echeta, I., Feng, X., Dutton, B., Leach, R., and Piano, S., 2020, “Review of Defects in Lattice Structures Manufactured by Powder Bed Fusion,” Int J Adv Manuf Technol, **106**(5–6), pp. 2649–2668.

[23] Li, C., Liu, J. F., Fang, X. Y., and Guo, Y. B., 2017, “Efficient Predictive Model of Part Distortion and Residual Stress in Selective Laser Melting,” Additive Manufacturing, **17**, pp. 157–168

[24] Subedi, S. C., Shahba, A., Thevamaran, M., Thoma, D. J., and Suresh, K., 2022, “Towards the Optimal Design of Support Structures for Laser Powder Bed Fusion-Based Metal Additive Manufacturing via Thermal Equivalent Static Loads,” Additive Manufacturing, **57**, p. 102956

[25] Kirkpatrick, S., Gelatt, C. D., and Vecchi, M. P., 1983, “Optimization by Simulated Annealing,” Science, **220**(4598), pp. 671–680.

[26] Campbell, M. I., Amon, C. H., and Cagan, J., 1997, “Optimal Three-Dimensional Placement of Heat Generating Electronic Components,” Journal of Electronic Packaging, **119**(2), pp. 106–113.

[27] Xiaohui, J., Chunbo, Y., Honglan, G., Shan, G., and Yong, Z., 2022, “Effect of Supporting Structure Design on Residual Stresses in Selective Laser Melting of AlSi10Mg,” Int J Adv Manuf Technol, **118**(5–6), pp. 1597–1608.

[28] Holmberg, E., Torstenfelt, B., and Klarbring, A., 2013, “Stress Constrained Topology Optimization,” Struct Multidisc Optim, **48**(1), pp. 33–47.

[29] Sulaiman, S., Hamouda, A. M. S., Abedin, S., and Osman, M. R., 2000, “Simulation of Metal Filling Progress during the Casting Process,” Journal of Materials Processing Technology, **100**(1), pp. 224–229.

References

[30] Zhang, Z.-D., Ibhadode, O., Ali, U., Dibia, C. F., Rahnama, P., Bonakdar, A., and Toyserkani, E., 2020, "Topology Optimization Parallel-Computing Framework Based on the Inherent Strain Method for Support Structure Design in Laser Powder-Bed Fusion Additive Manufacturing," Int J Mech Mater Des, **16**(4), pp. 897–923.

[31] Misiun, G., van de Ven, E., Langelaar, M., Geijselaers, H., van Keulen, F., van den Boogaard, T., and Ayas, C., 2021, "Topology Optimization for Additive Manufacturing with Distortion Constraints," Computer Methods in Applied Mechanics and Engineering, **386**, p. 114095.

[32] Liang, X., Cheng, L., Chen, Q., Yang, Q., and To, A. C., 2018, "A Modified Method for Estimating Inherent Strains from Detailed Process Simulation for Fast Residual Distortion Prediction of Single-Walled Structures Fabricated by Directed Energy Deposition," Additive Manufacturing, **23**, pp. 471–486.

[33] Chen, Q., Liang, X., Hayduke, D., Liu, J., Cheng, L., Oskin, J., Whitmore, R., and To, A. C., 2019, "An Inherent Strain Based Multiscale Modeling Framework for Simulating Part-Scale Residual Deformation for Direct Metal Laser Sintering," Additive Manufacturing, **28**, pp. 406–418.

[34] Shaikh, A. S., Schulz, F., Minet-Lallemand, K., and Hryha, E., 2021, "Microstructure and Mechanical Properties of Haynes 282 Superalloy Produced by Laser Powder Bed Fusion," Materials Today Communications, **26**, p. 102038.

[35] Miki, T., and Yamada, T., 2021, "Topology Optimization Considering the Distortion in Additive Manufacturing," Finite Elements in Analysis and Design, **193**, p. 103558.

[36] Setien, I., Chiumenti, M., van der Veen, S., San Sebastian, M., Garciandía, F., and Echeverría, A., 2019, "Empirical Methodology to Determine Inherent Strains in Additive Manufacturing," Computers & Mathematics with Applications, **78**(7), pp. 2282–2295.

[37] Boos, E., Ihlenfeldt, S., Milaev, N., Bruns, M., and Elsner, B. A. M., 2023, "Simulation-Based Support Generation for Laser Powder Bed Fusion Processes," 3D Printing and Additive Manufacturing, p. ahead of print.

[38] Vaidya, R., and Anand, S., 2016, "Optimum Support Structure Generation for Additive Manufacturing Using Unit Cell Structures and Support Removal Constraint," Procedia Manufacturing, **5**, pp. 1043–1059

Manufacturing of Metal Components[a]

Manufacturing Method	Pros	Cons	Examples
Conventional Manufacturing (Subtractive in nature)	✓ Mass Manufacturing ✓ Mature	− Simple geometry − High material waste − Specialized tooling	• Milling • Die-casting • Laser cutting
Additive Manufacturing (Additive in nature)	✓ Complex geometry ✓ Reduced delivery costs ✓ Inventory stock reduction ✓ Mass customization ✓ No specialized tooling	− Initial start-up costs − Limited materials − Slow build time	• Directed Energy Deposition • Material Extrusion • Powder Bed Fusion

b

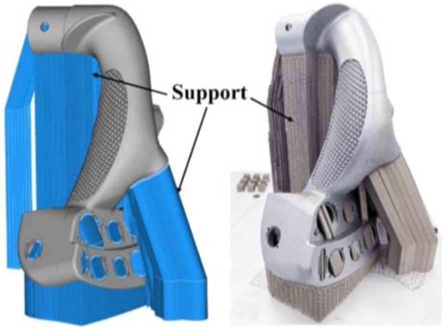

c

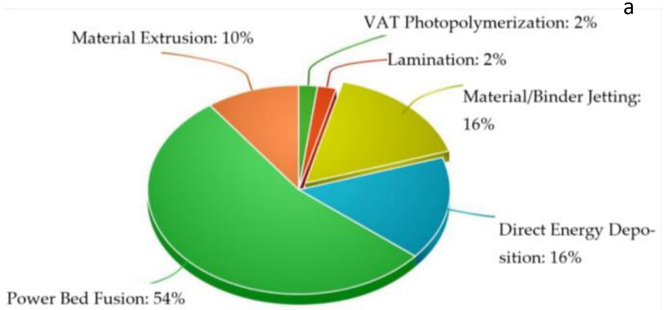

a

a. Vafadar et. al (2021) b. Tucker et. al (2016) c. Wang, D., et.al (2022)

Geometric Inaccuracy: Residual Stress

- Thermal Cycle[3]
  - Rapid heating with steep gradients
  - Rapid solidification with high cooling
  - Melt-back involving simultaneous melting and remelting

Block shell support[4]

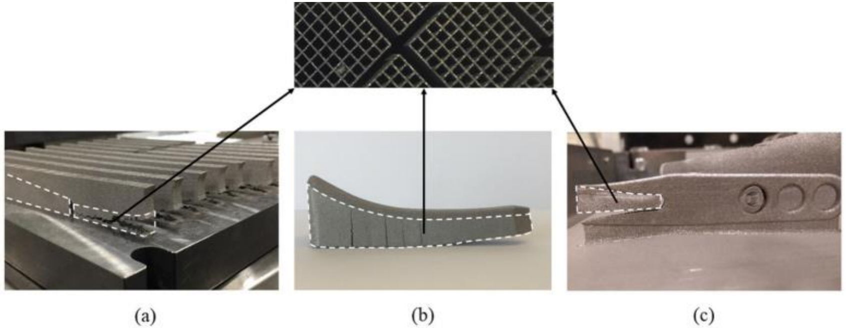

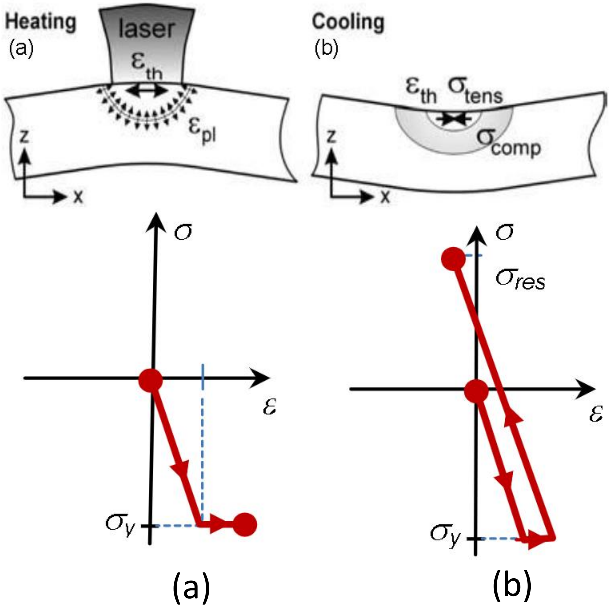

Model of one layer of stress for laser powder bed fusion (a) Heating phase and (b) cooling phase[3]

3. Li, C., et. al (2018)   4. Cheng, L., et. al (2019)

Support Structures

Purpose[5,9]:

- **Dissipate Heat**[6,9,10]
- Maintenance of structural integrity[4,7,11]

Methods to generate Support structures

- Topology Optimization for arbitrary states[6,7,11]
- Lattice Structures[5,8-10]

Cantilever Beam[6,7]

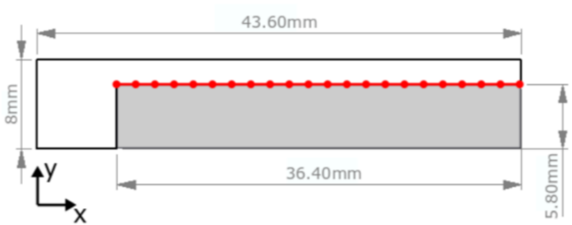

Design for heat dissipation[6]

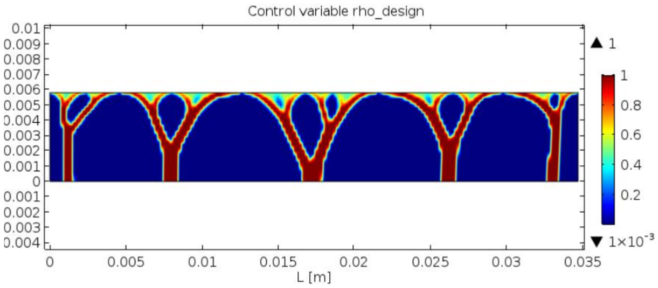

Design for structural compliance[7]

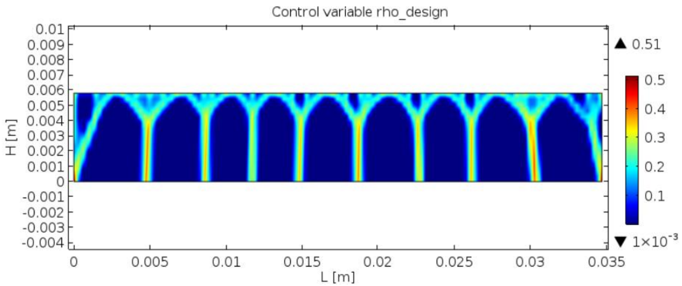

5. Jiang, J, et. al (2018) 6. Bartsch, K., et. al (2019) 7. Bartsch, K., et. al (2018) 8. Miki, T. and Nishiwaki, S., (2022) 9. Huang, R., et. al (2020) 10. Lee, K.H., et.al (2022) 11. Pellens, J., et.al (2020)

Gradient-Based Optimizers

Pros:

- Faster convergence
- Local solution search

Cons:

- More likely to get in a local optima
- Require differentiable design variables

Examples:

- Gradient Descent
- Method of Moving Asymptotes

Applications in Lattice Support Structure Design :

- Minimizing compliance
- Minimizing mean temperature
- Minimizing temperature gradient

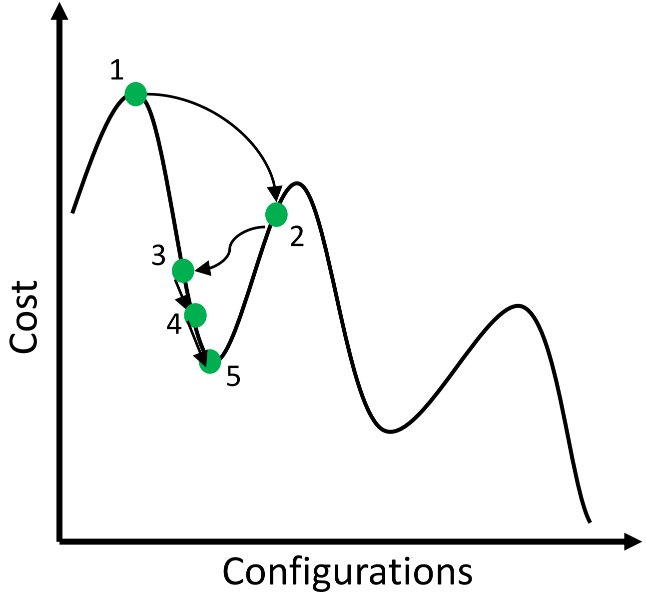

Non-Gradient-Based Optimizers

Pros:

- Do not require differentiable design variables
- Ideally a global solution search

Cons:

- Computationally expensive

Examples:

- Genetic Algorithms
- Simulated Annealing

Applications in Lattice Support Structure Design :

- Minimizing compliance

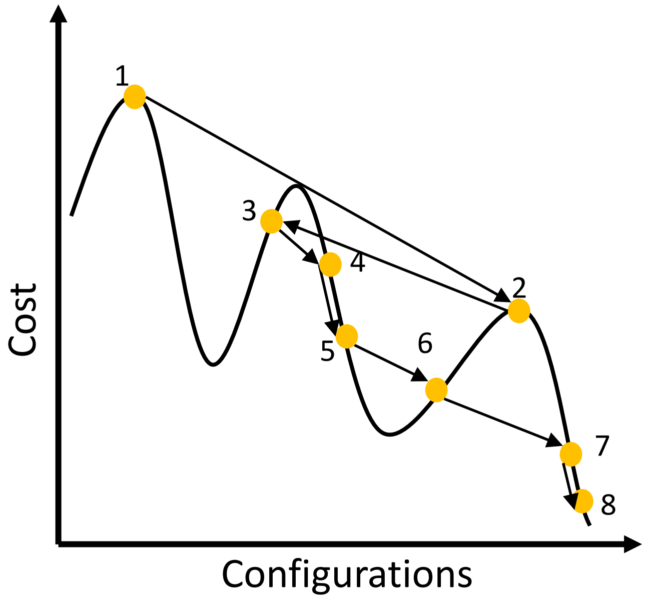

h. Eberhard, P., et al (1999)   i. Porter, J., et al (2009)   j. Gosselin,L., et al (2009)

Lattices

Artificial microscopic structures with strategically designed geometry to control properties on the macroscopic level[12,13]

Lattice Support Structures[12-14]

- Self-supporting structure
- Light-weight design
- Tailorable physical properties
- Ease of powder removal

Lattice Structures in Nature[12]

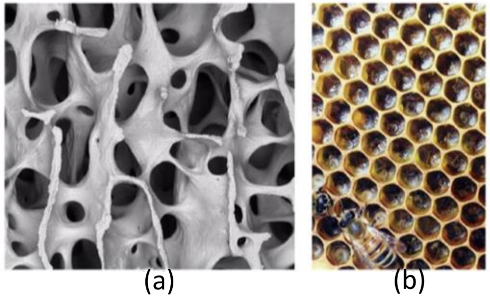

Lattice Structures for AM

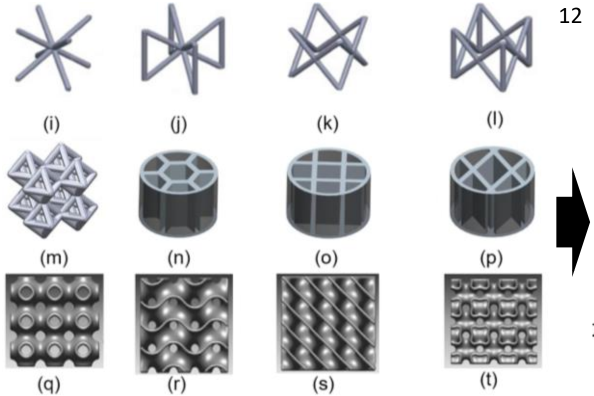

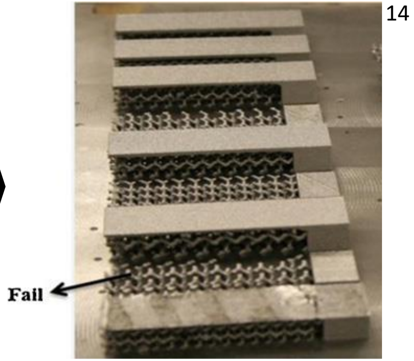

12. Nazir, A., et. al (2019) 13. Liang, H et. al (2011) 14. Hussein, A., et. al (2013)

Existing Gradient-Based-Optimizers

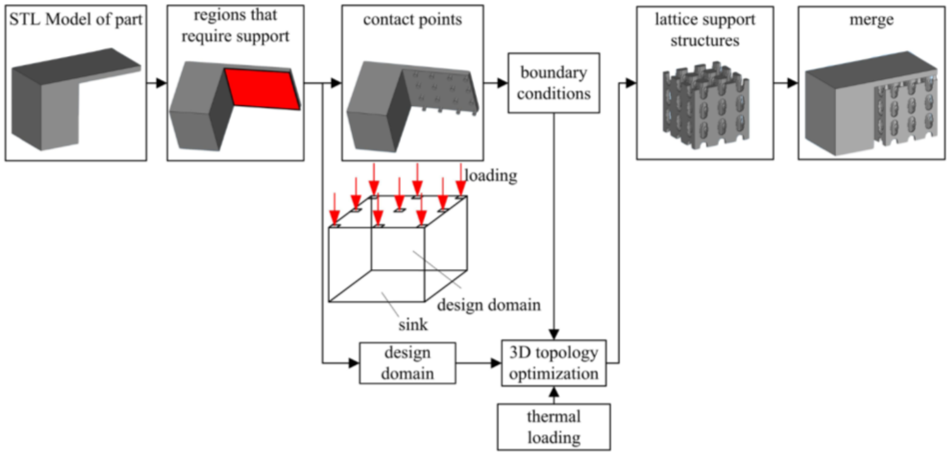

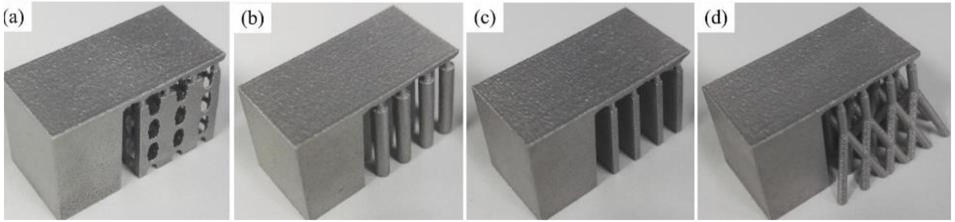

Optimizer: Method of Moving Asymptotes

Problem

Minimize thermal compliance w.r.t material elements

s.t. volume

Advantages:

- Fast evaluation using homogenization approximation
- Least amount of vertical warpage than the standard designs (b-d)

Disadvantages:

- Does not consider spatio-temporal inhomogenization

d. Huang, R., et. al (2020)

Existing Gradient-Based-Optimizers

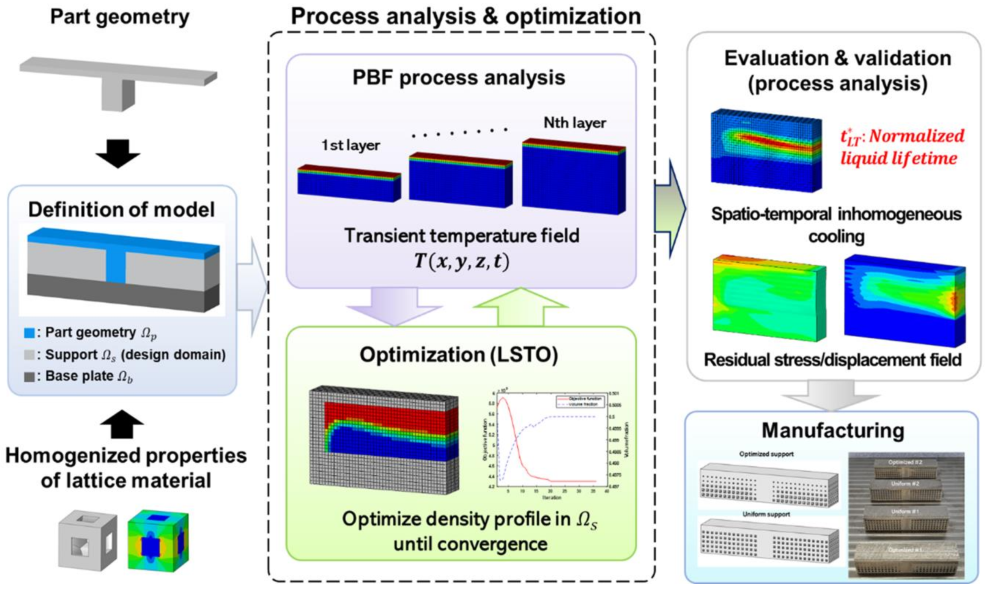

Optimizer: Method of Moving Asymptotes

Problem:

Minimize temperature gradient w.r.t cell density

s.t. volume

Advantages:

- Fast evaluation using homogenization approximation
- Captures spatio-temporal homogenization
- 47% reduced stress

Disadvantages:

- Sensitivity Analysis Approximations
- Demonstrated only on simple geometry
- Limited consideration of Design Constraints

e. Lee et.al (2022)

Existing Non-Gradient-Based Optimizers

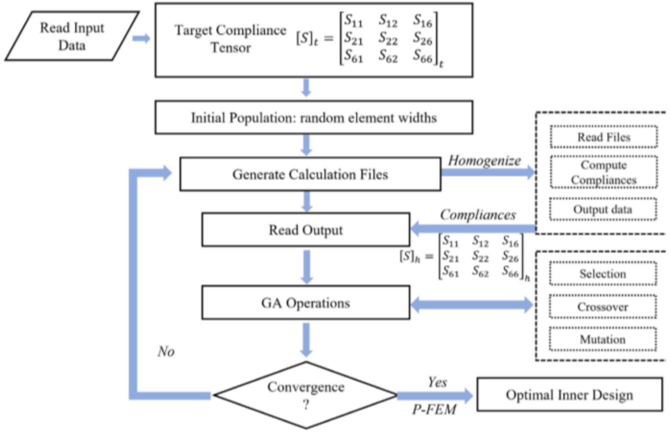

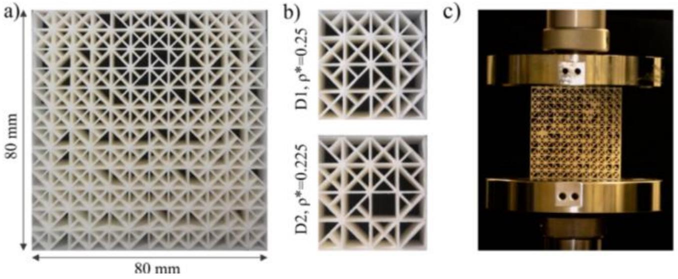

Optimizer: Genetic Algorithm

Problem:

Minimize structural compliance w.r.t cell geometry

s.t. volume

Advantages:

- Fast evaluation using homogenization approximation
- Hybrid lattice structures

Disadvantages:

- Only planar optimization
- Does not consider use as metal support structure

f. Reis D.F. and Karathanasopoulos, (2022)

Existing Optimizer Method to Design Heat Dissipating Lattice Support Structures

Optimize periodic unit cell[9,14]

- Minimize thermal compliance[9]
  - •Did not consider non-uniform heat distribution

Optimized support

Traditional supports

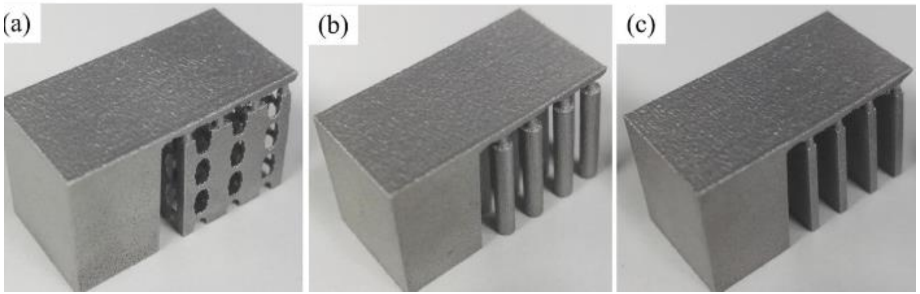

Optimize density distribution[4,10,11,19]

- Minimize thermal gradient w.r.t density[17]
  - •Accumulated error from approximations
  - •Limited AM constraints

a)

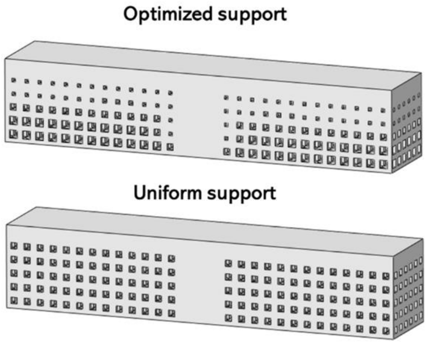

b)

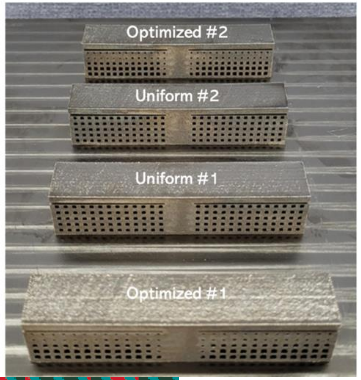

4. Cheng, L., et. al (2019) 9. Huang, R., et. al (2020) 10. Lee, K.H., et.al (2022) 11. Pellens, J., et.al (2020) 14. Hussein, A., et. al (2013) 19. Cheng, L., et. al (2018)

Existing Designs for Lattice Support Structures Connection to Complex Geometries

Block shell support[3]

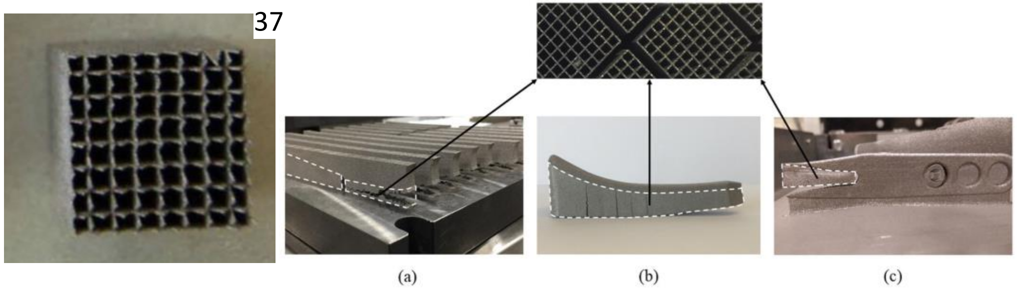

Non-Solid Connections

- ✓ Reduced material cost
- ✓ Easily removable
- ✓ Found in commercial software
- – Poor for large overhangs
- – Trap unused powder

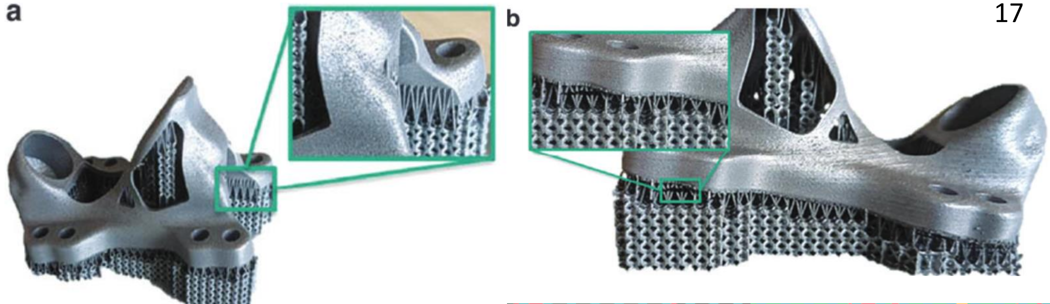

Pin Connections

- ✓ Increased connection to part
- ✓ Simple geometry
- – High computational cost to optimize

3. Cheng, L., et. al (2019) 37. Krol, T.A., et. al (2012) 17. Boos, E., et. al (2022)

Existing Designs for Lattice Support Structures Connection to Flat Geometries

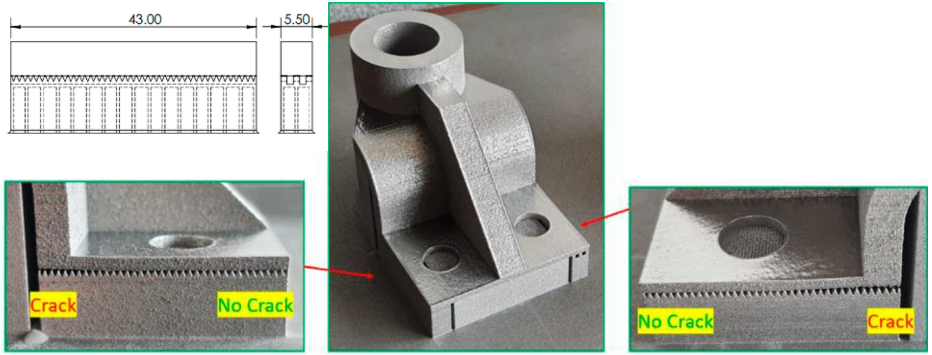

B2 on the left

Bracket B

B1 on the right

Tooth Connections

- ✓ Reduced material cost
- ✓ Easily removable
- – Reduced flexibility on spacing
- – Not shown to work with hybrid lattices

Research Gaps

1. Restricting types of manufacturable unit cells limits the types of AM constraints that can be considered, such as using a varying density of a simple cubic cell

2. Nondifferentiable lattices make it difficult for gradient-based optimizers to fully explore the design space and can lead to inaccuracies due to accumulating approximations.

3. High computation time is a major limitation for using non-gradient-based optimizers, particularly with powerful methods such as simulated annealing (SA).

Defining Constraints

Volume

Material Waste

- Support structure is sacrificial for LPBF
- Cost of powder

Build time

- Laser scanning

Interfacial area

- Post-processing costs
    - Existing methods
- Surface roughness
    - cost
- Thin features

Removal of support structure by depth of cut $(a_p)^k$:

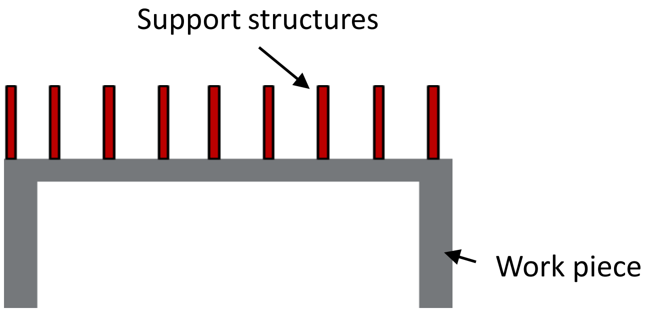

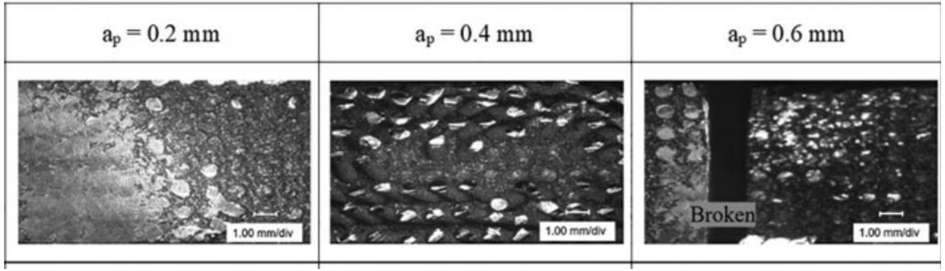

0.3mm strut thickness

k. Cao, Q. et. al (2022)

Equivalent Flash Heating Method

Heating

$$\begin{cases} \rho c \dfrac{dT_i(t,x)}{dt} = \nabla \cdot \left(\mathrm{k}\nabla T_i(t,x)\right) + q(\boldsymbol{x}) & \text{in } (0,t_h)\times\Omega_A \\ -\left(\mathrm{k}\nabla T_i(t,x)\right)\cdot n = h\nabla T_i(t,x) & \text{on } (0,t_h)\times\Omega_A/\Omega \\ T_i(t,\boldsymbol{x}) = T_{base} & \text{on } (0,t_h)\times\Omega_b \\ T = T_{powder} & \text{In } \varphi_A \end{cases}$$

Cooling

$$\begin{cases} \rho c \dfrac{dT_i(t,x)}{dt} = \nabla \cdot \left(\mathrm{k}\nabla T_i(t,x)\right) + q(\boldsymbol{x}) & \text{in } (0,t_c)\times\Omega_A \\ -\left(\mathrm{k}\nabla T_i(t,x)\right)\cdot n = h\nabla T_i(t,x) & \text{on } (0,t_c)\times\Omega_A/\Omega_b \\ T_i(t,\boldsymbol{x}) = T_{base} & \text{on } (0,t_c)\times\Omega_A/\Omega_b \\ T = T_{powder} & \text{in } (0,t_c)\times\Omega_A \end{cases}$$

$$q(\boldsymbol{x}) = \begin{cases} q & \text{for } x\in\Omega_I \\ 0 & \text{otherwise} \end{cases}$$

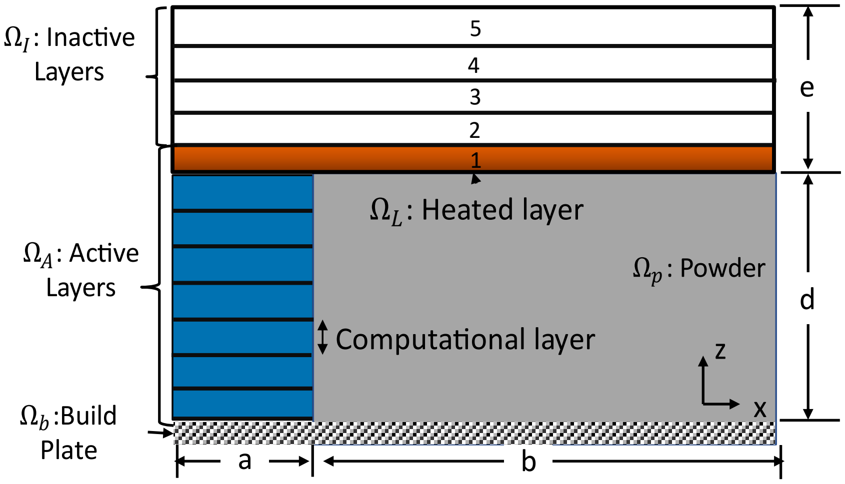

Equivalent Flash Heating Method

Process Parameter	Value
Volume heat flux, q $[W/m^3]$	1.96×10^{13}
Convection Coefficient for heat loss to environment, h_{side} $[W/m^2°C]$	100
Convection Coefficient for heat loss to build plate, h_{plate} $[W/m^2°C]$	8000
Heating time per layer, t_h[s]	4×10^{-4}
Cooling time per layer, t_c [s]	5
Build plate temperature, T_{amb} [°C]	20
Inherent strain vector in x, y, z	-0.016,-0.016, 0.014

Cantilever Beam

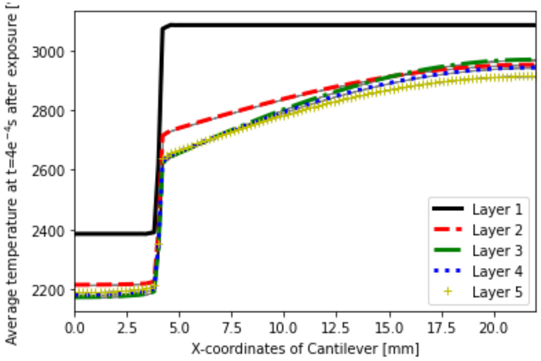

Aerospace Bracket

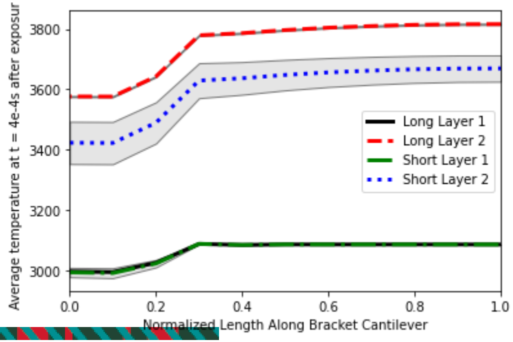

Equivalent Flash Heating Method

Heating

Cooling

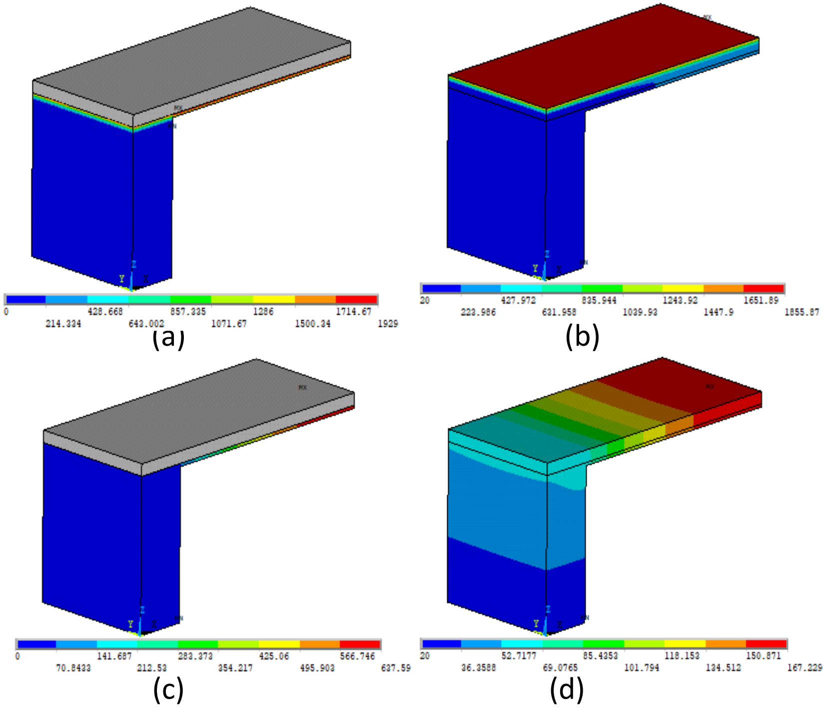

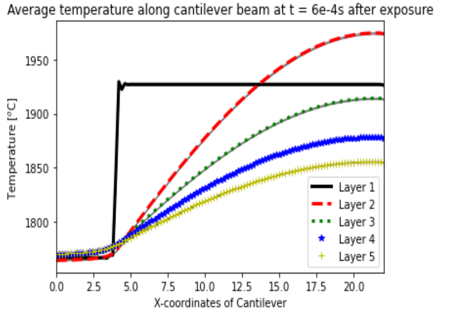

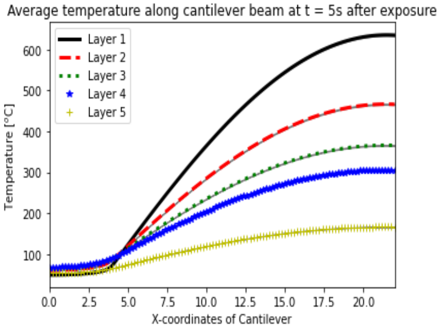

Case Study of Cantilever Beam: Validation

Iteration History of 30 runs

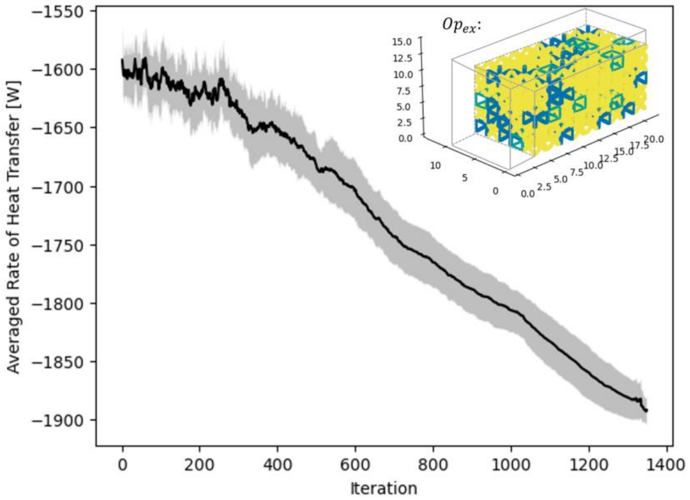

Op_{ex}: Objective = -1,900 W, Volume = 615 mm^3, Area = 106 mm^2.

Stages	Traditional SA	M-SAM
Exploration	1	Total
Intermediate	1	Total/100
Fine-Tuning	1	Total/200

Analysis Model	Simulation	SC Only	BV Only	FC Only	Op_{ex}
Steady-state	$Q_{in,h}$[W]	-1,196	-1,607	-2,124	-1,608
	$Q_{in,exact}$[W]	-1,198	-1,605	-2,132	-1,647
Transient	t_s[s]	3.25	2.18	1.38	1.45

Case Study of Cantilever Beam

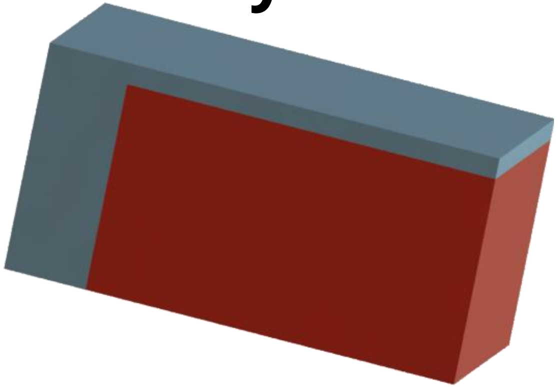

Design variables: 225
possible configurations: 3^{225}
Evaluation time per iteration: ~3s

SA Hyperparameters: $T_0 = 50$; $\alpha = 0.5$
$V_{max} = 0.4*V_{solid} \approx 750\ mm^3$
$A_{max} = 0.55*A_{solid} \approx 140\ mm^2$
$\sigma^{PN}_{Max} = 1/1.5 = 0.66$
$U_{z,max} = Layer/\rho_{shr} = 32\ \mu m$

Iteration History of 30 runs

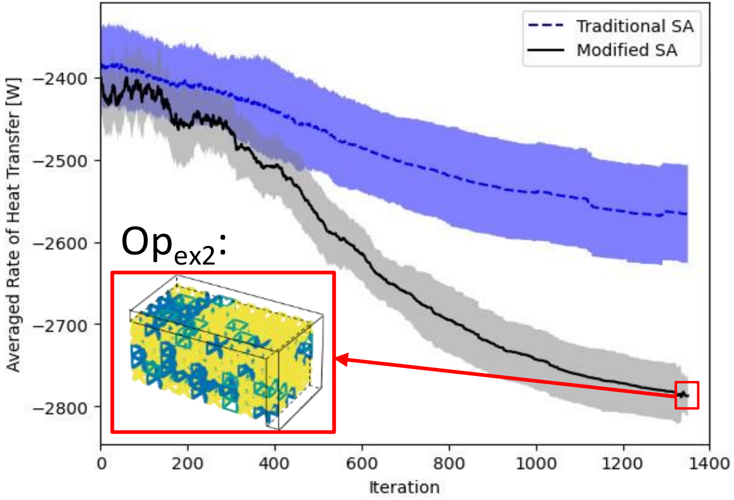

Stages	Traditional SA	M-SAM
Exploration	1	Total
Intermediate	1	Total/100
Fine-Tuning	1	Total/200

Case Study of Aerospace Bracket

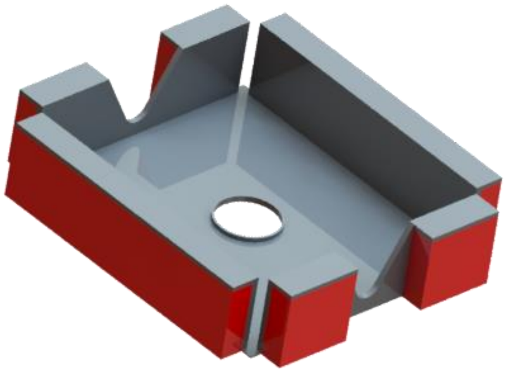

Design variables: 1,776
possible configurations: $3^{1,776}$
Evaluation time per iteration: ~3s

SA Hyperparameters: $T_0 = 50$; $\alpha = 0.5$
$V_{max} = 0.4 * V_{solid} \approx 5{,}900\ mm^3$
$A_{max} = 0.55 * A_{solid} \approx 1360\ mm^2$
$\sigma^{PN}_{Max} = 1/1.5 = 0.66$
$U_{z,max} = Layer/\rho_{shr} = 76\ \mu m$

Iteration History of 30 runs

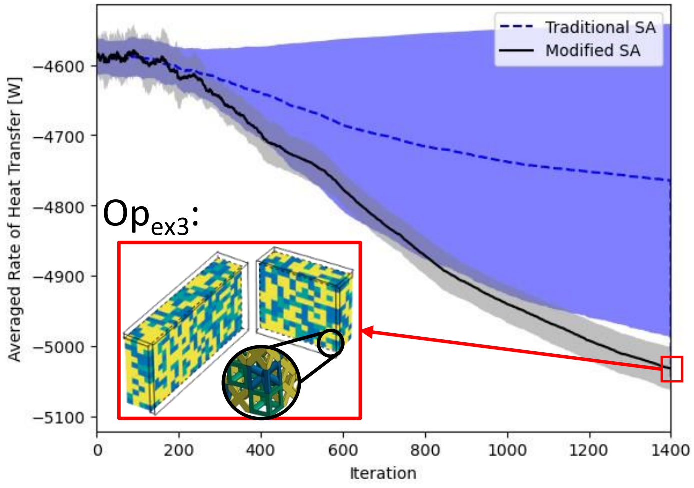

Stages	Traditional SA	M-SAM
Exploration	17	Total
Intermediate	17	Total/100
Fine-Tuning	17	Total/200

Asymptomatic Homogenization

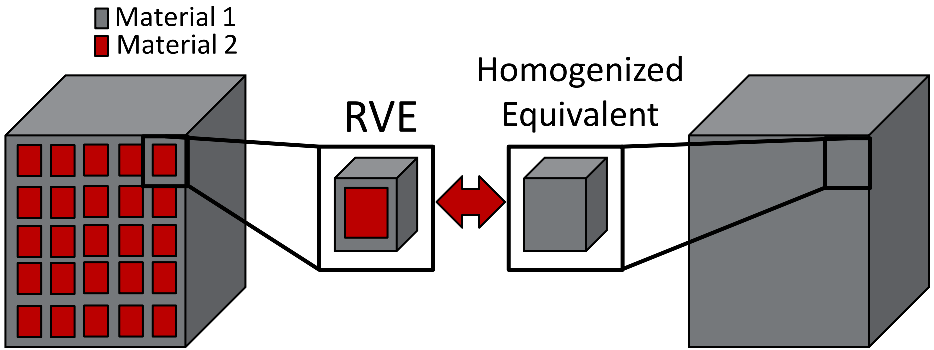

Let y=x/β

Double-scale asymptotic expansion

$$\underbrace{T(x,y)}_{\text{Exact Solution}} = \underbrace{T_0(x,y)}_{\text{Average}} + \underbrace{\beta T_1(x,y) + \beta^2 T_2(x,y) + \ \ldots}_{\text{Pertubations from microstructure}}$$

Governing equations:

$$\begin{cases} k\nabla^2 T(x,y) + f = 0 & \text{(Steady-state heat)} \\ q(x,y) = -k\nabla T(x,y) & \text{(Fourier's Law)} \end{cases}$$

Effective thermal conductivity (K_{ijkl}^{eff})

$$K_{ijkl}^{eff} = \frac{1}{V_{RVE}} \int_{V_{RVE}} K_{ijmn} M_{mnkl} d$$

Conductivity of unit cell (K_{ijmn})

Structure Tensor (M_{mnkl})

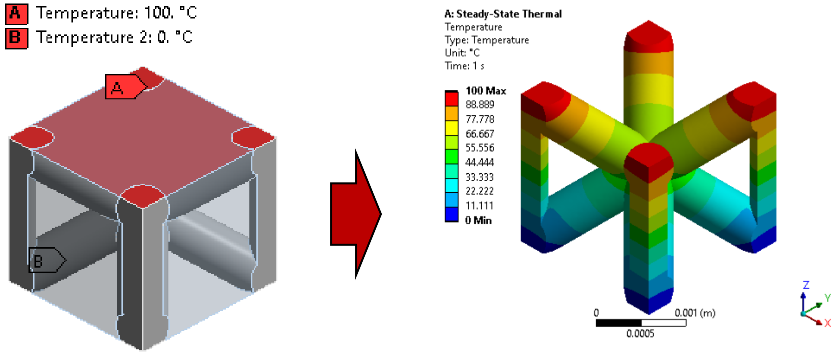

P-Norm Stress

$$\sigma_j^{PN}(x) = \left(\frac{1}{N_j}\sum_{a\in\Omega_j}\left(\sigma_a^{vM}(x)\right)^p\right)^{\frac{1}{p}}$$

$$\overbrace{\sigma_1 \geq \sigma_2 \geq \cdots \geq \sigma_{\frac{n_e}{n_c}}}^{\text{Cluster 1}} \geq \overbrace{\cdots \geq \sigma_{\frac{2n_e}{n_c}}}^{\text{Cluster 2}} \geq \overbrace{\cdots \geq \sigma_{n_e}}^{\text{Cluster } n_c}$$

- Minimizes stress concentrations
- Global and local search
- Stress-level technique
- $\sigma_j^{PN} > \sigma_y$:= plastic deformation
- $\sigma_j^{PN} < \sigma_y$:= elastic deformation

Die Casting

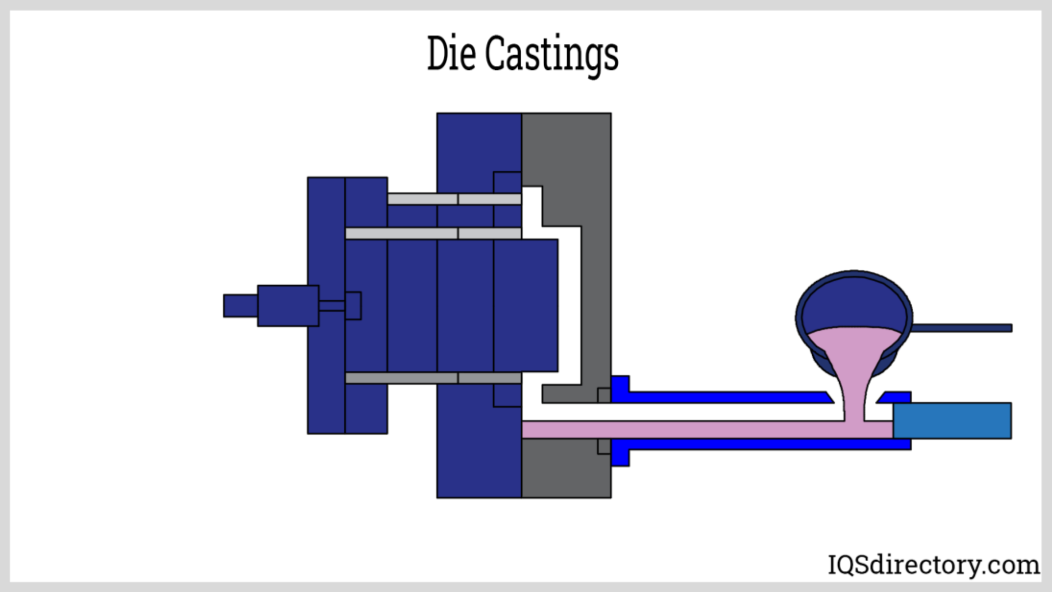
Die Castings
IQSdirectory.com

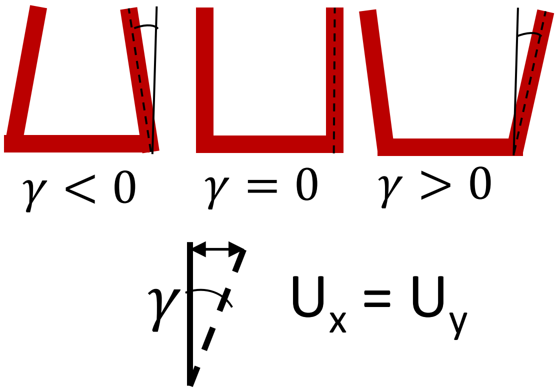
Draft Angle (γ)
$\gamma < 0$
$\gamma = 0$
$\gamma > 0$
γ
$U_x = U_y$

Inherent Strain Method (ISM)

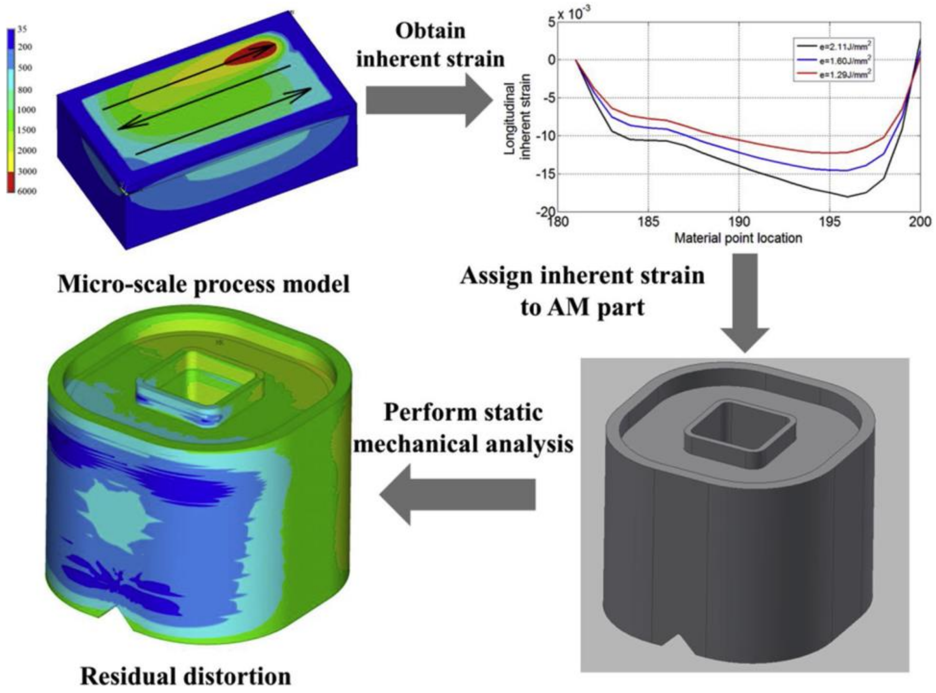

Multiscale Framework

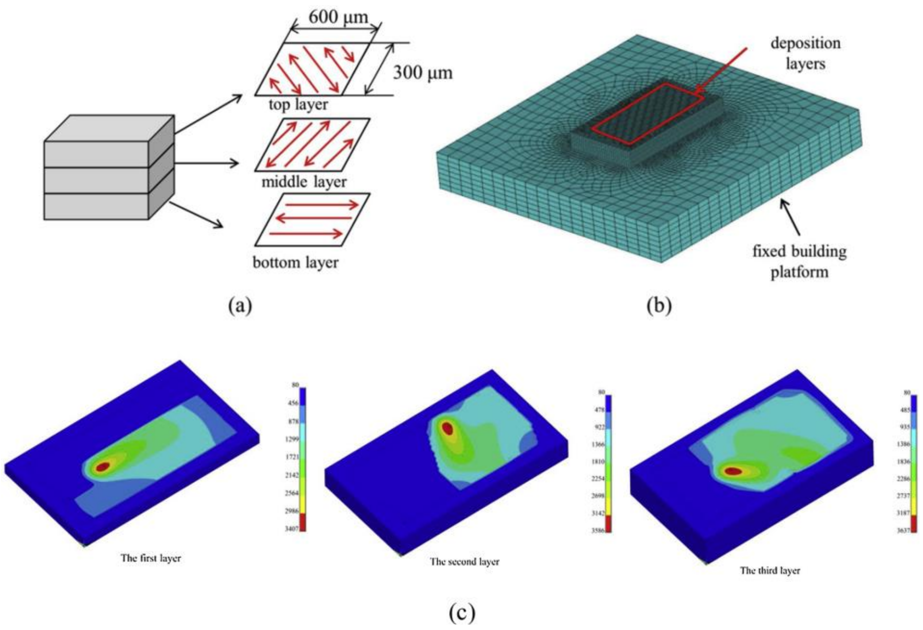

Thermomechanical model

33. Chen, Q., et. al (2019)

Inherent Strain Method (ISM)

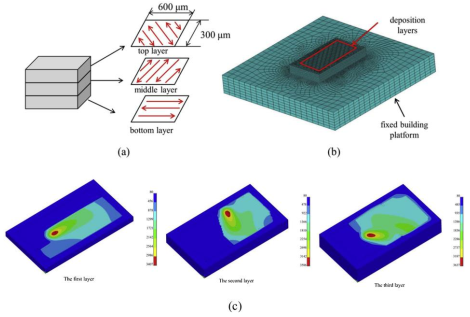

$$\varepsilon^{inh} = \begin{cases} \varepsilon_{xx} \\ \varepsilon_{yy} \\ \varepsilon_{zz} \end{cases}$$

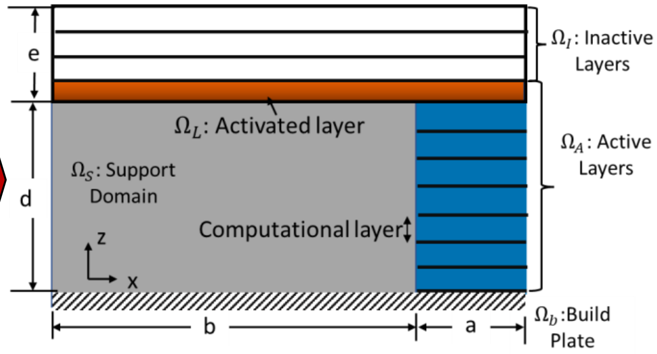

Governing equation:

$$\begin{cases} \nabla \cdot \sigma_i = 0 \\ \sigma_i = \mathbf{C}\varepsilon_e^i \\ \varepsilon_{tot}^i = \varepsilon_e^i + \varepsilon_p^i + \varepsilon_{in}^i, \end{cases}$$

Inherent Strain Method

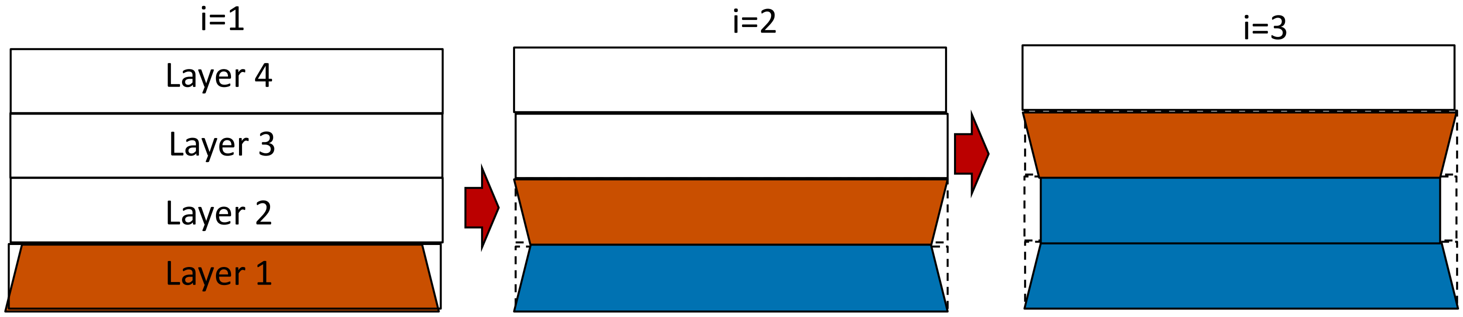

33. Chen, Q., et. al (2019)

ISM of Bracket

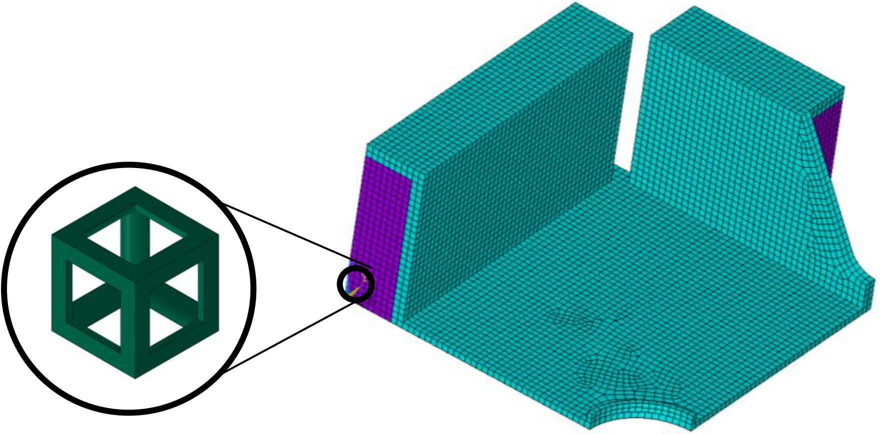

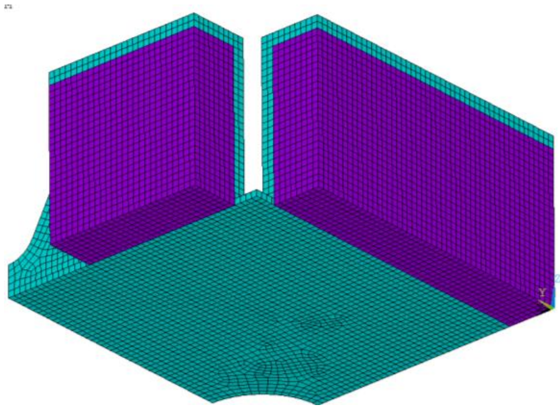

Step 4

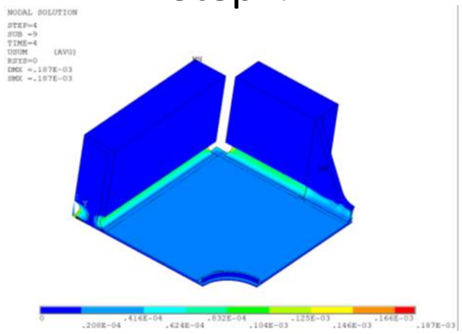

Step 15

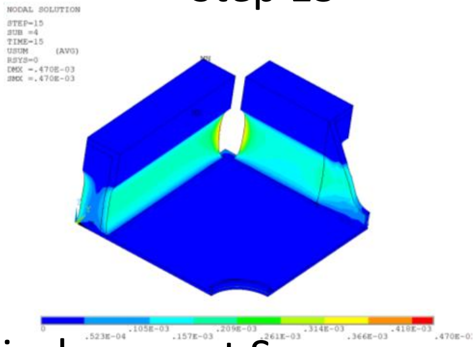

Step 26

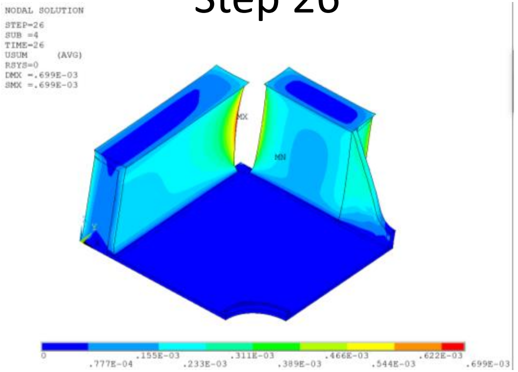

Displacement Sum

Equivalent Static Load Sub-models

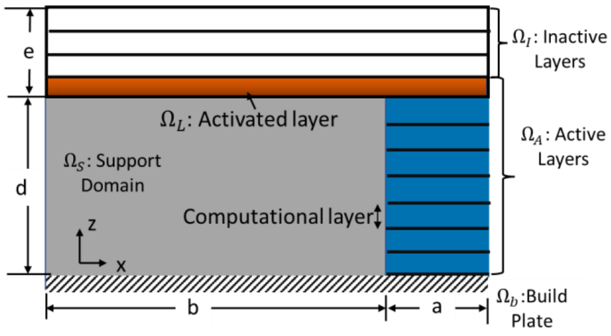

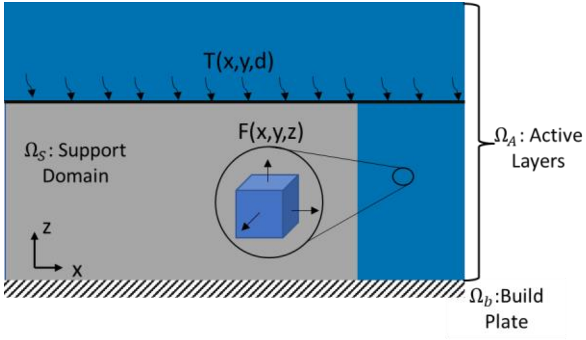

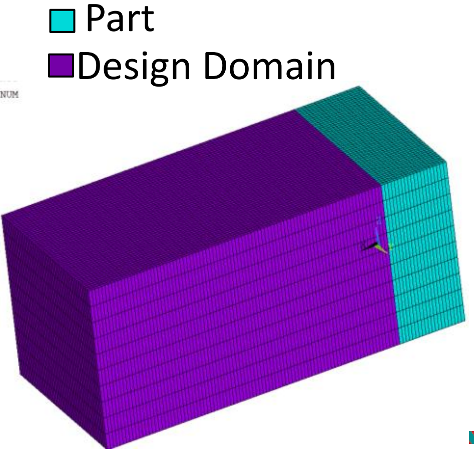

Steady-State Thermal

Governing equation:

$$\begin{cases} \nabla \cdot (K \nabla \boldsymbol{T}) + \boldsymbol{q} = 0 \\ T(x,y,0) = T_{base} \\ T(x,y,d) = T_{source} \end{cases}$$

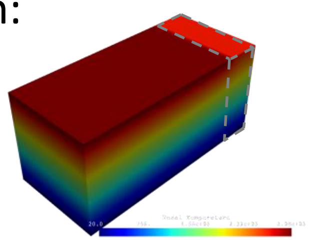

Example Temperature Results

Static Structural

Governing equation:

$$\begin{cases} \nabla \cdot \sigma + F = 0 \\ U(x,y,0) = 0 \end{cases}$$

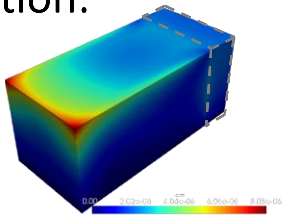

Example Displacement Results

Case Study of Aerospace Bracket

Iteration History of 30 runs

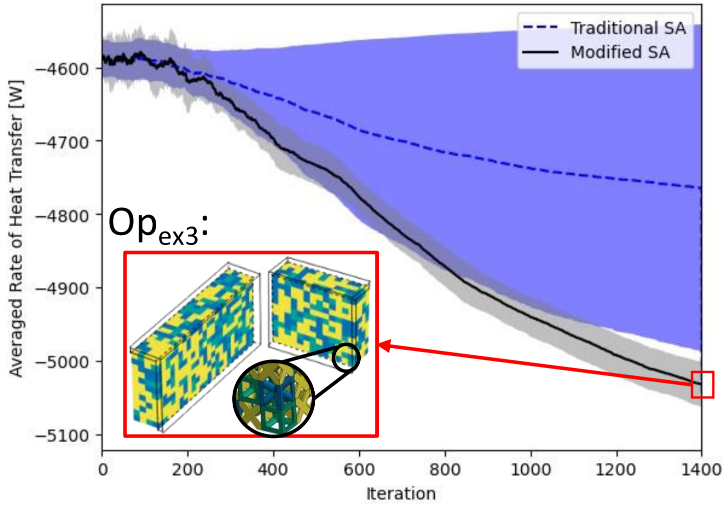

Objective = -5,039 W, Volume = 5,481 mm^3, Area = 1,243 mm^2, p-Norm = 0.648, U_{sum} = 69.7 mm

Comparison of support designs*

	$\lvert Q_{in}\rvert$	V(x)	A(x)	P-norm Stress	Max(U_{sum}) [μm]	SC/BV/FC	V(x) < 5,900 A(x) < 1,360 P-norm < 0.66 Max(U_{sum})< 76
Solid	12,479	14,208	2,368	0.609	14	--	No
SC Only	3,524	3,232	1,367	0.648	96.0	1,776/0/0	No
BV Only	4,624	5,008	[illegible]	0.648	97.5	0/1,776/0	No
FC Only	6,004	6,553	1,568	0.637	74.7	0/0/1,776	No
$Op_{avg,3}$	**4,902 (29.4)**	**5,315 (36.2)**	**1,222 (13.7)**	**0.643 (0.0037)**	**72.8 (2.3)**	**388/589/799 (16/20/30)**	**Yes**

Satisfies Constraints

Average of ~60% Material Cost

Average of ~47% Post-processing Cost

*standard deviation in ( )

Cost Comparison

Cost of Haynes 282[39]: $145/kg

$\rho_{Haynes282}$: 8.29 g/cm^3

Cost Savings (Solid Support)

$13,527*

34. Xiaohui, J., et. al (2022) 35. Atzeni, E., and Salmi, A., (2012)

*1,000 brackets printed

Reducing Material Waste using Multi-Sized Unit Cells

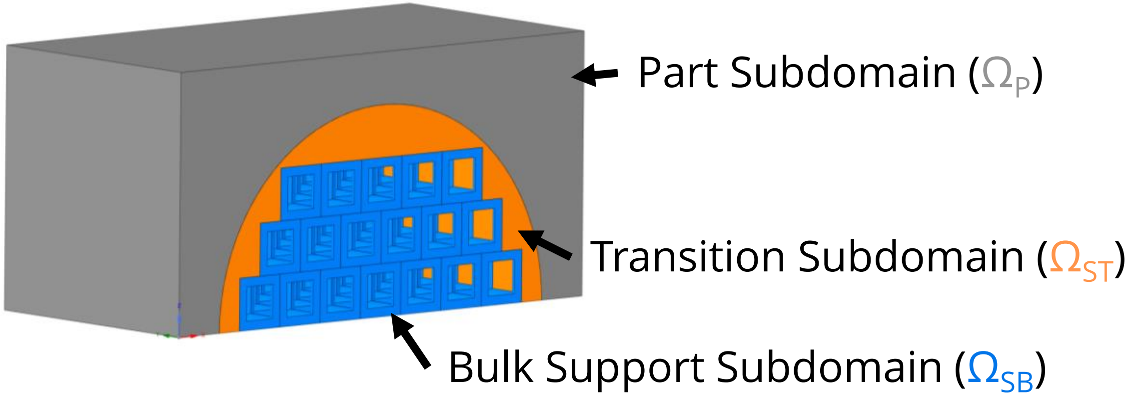

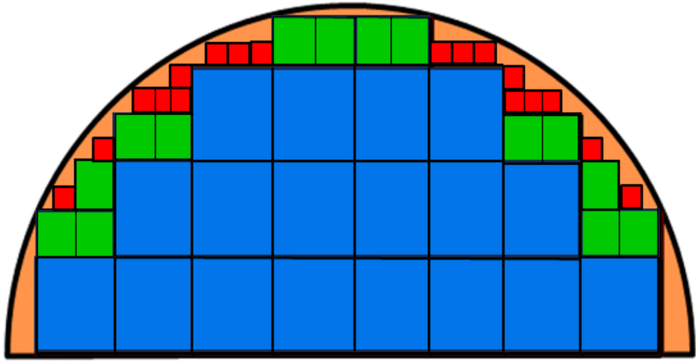

Multi-Sized Unit Cells

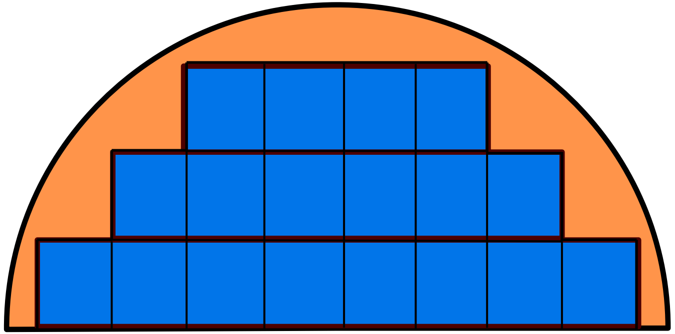

Single Sized Unit Cells

Unit Cell Size	Pros	Cons
Large	✓ Decrease volume ✓ Reduce build time	– Decrease strength – Do not fit in transition
Small	✓ Increase stiffness ✓ Reduce volume	– Increase volume – Increase build time

Case Study of Heat Exchanger Adapter

Iteration History of 30 runs

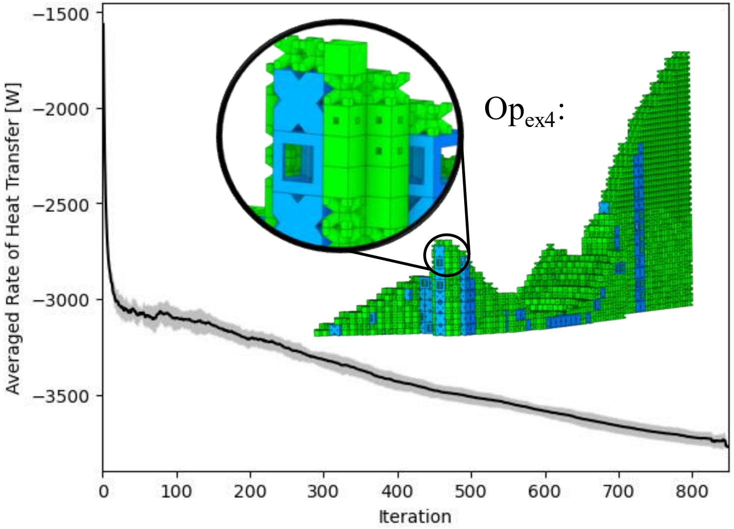

Objective = -3,742 W, Volume = 3,807mm^3, p-Norm = 0.08, U_{sum} = 18.24 mm

Comparison of support designs*

	$\lvert Q_{in} \rvert$	V(x)	P-norm Stress	Max(U_z) [μm]	SC/TR/FC sc/bv/sol	V(x) < 3,808 P-norm < 0.66 Max(U_z)< 40
Solid	6,470	7,617	0.053	4.6	--	No
SC Only	3,182	**3,711**	0.166	19.45	631/0/0 0/0/2,563	Yes
TR Only	3,756	4,468	0.108	13.0	0/631/0 0/0/2,563	No
FC Only	4,775	4,891	0.072	8.08	0/0/1,776 0/0/2,563	No
$Op_{avg,4}$	**3,734 (37)**	3,801 (9.6)	**0.087 (0.004)**	**16.0 (0.53)**	**151/185/295 645/1,228/689 (6/12/11/18/16/21)**	**Yes**

Satisfies Constraints

Average of ~51% Material Cost

*standard deviation in ( )

Cost Comparison

Cost of Haynes 282[39]: \$145/kg

$\rho_{Haynes282}$: 8.29 g/cm^3

Cost Savings (Solid Support)

\$1,301*

39. Ziev, T., et. al (2023)   *1,000 printed

Reducing Size + Forced Flat Domain

3 sizes:

10 mm

- Low volume
- Low compliance

5 mm

2.5 mm

- High volume
- High compliance

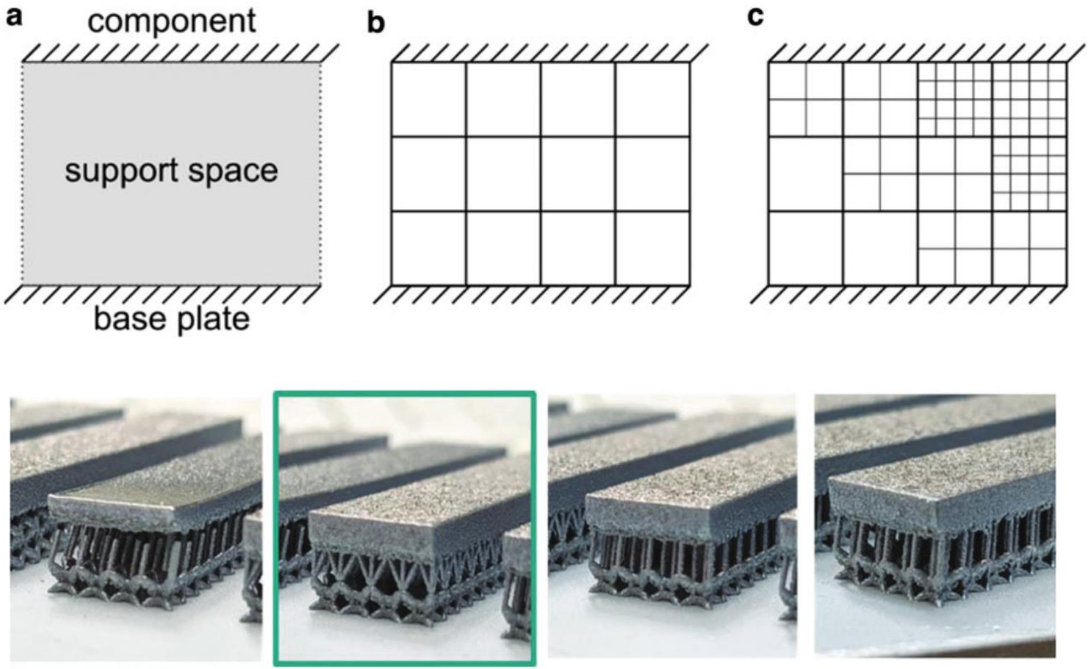

FIG. 5. Printed cantilever geometries to identify the required distribution of connection structures between unit cells and solids. The structure used for further design is highlighted *green*.

37. Boos, E., et. al (2022)

Case Study of Heat Exchanger Adapter

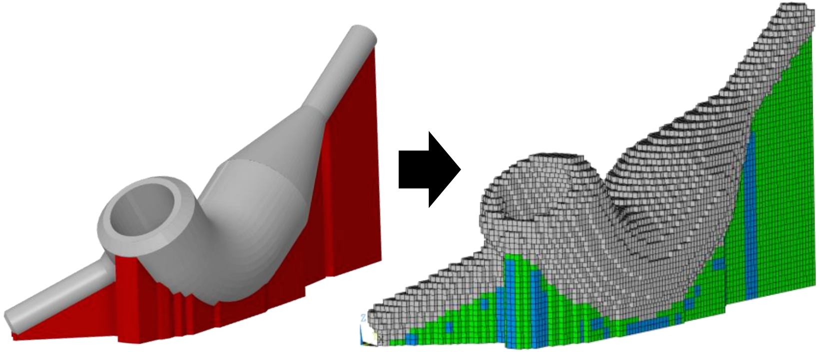

Design variables: 3,194 (631 2mm; 2,563 1mm)
possible configurations: $3^{631}\times3^{2,563}$
Evaluation time per iteration: ~3s

SA Hyperparameters: T_0 = 50; α = 0.5

$V_{max} = 0.5*V_{solid} = 3,808\ mm^3$

$\sigma^{PN}_{Max} = 1/1.5 = 0.66$

$U_{z,max}$ = Layer = 40 µm

Iteration History of 30 runs (M-SAM) and 12 runs (TSA)

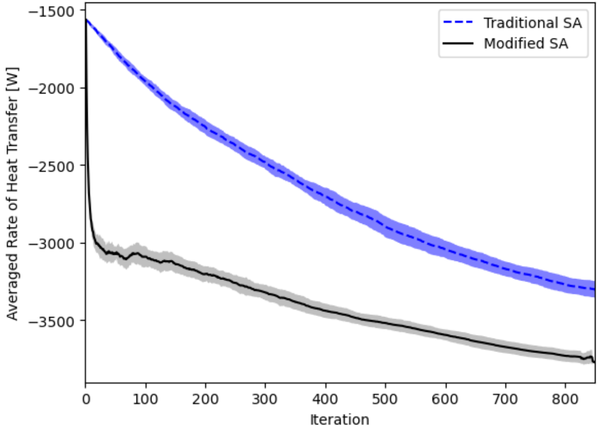

Stages	Traditional SA	M-SAM
Exploration	Total/400	Total/4
Intermediate	Total/400	Total/40
Fine-Tuning	Total/400	Total/400

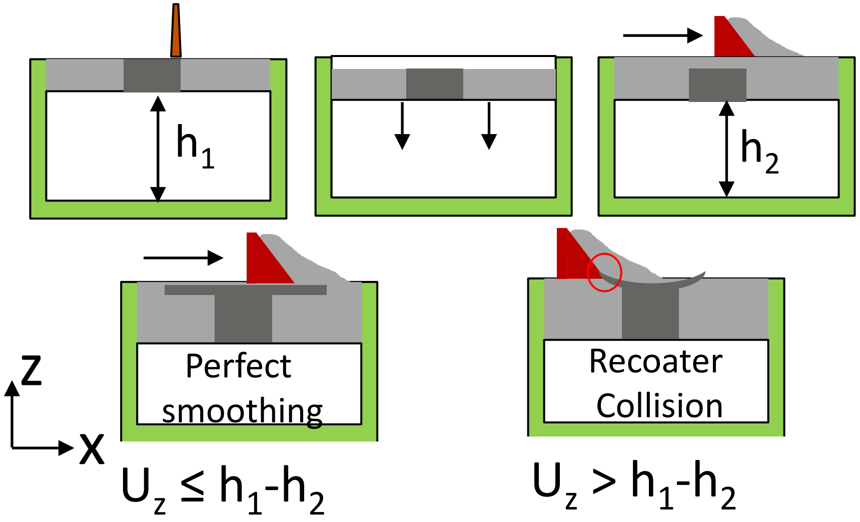
h1
h2
Perfect smoothing
Recoater Collision
Z
X
$U_z \leq h_1 - h_2$
$U_z > h_1 - h_2$


https://www.additivemanufacturing.media

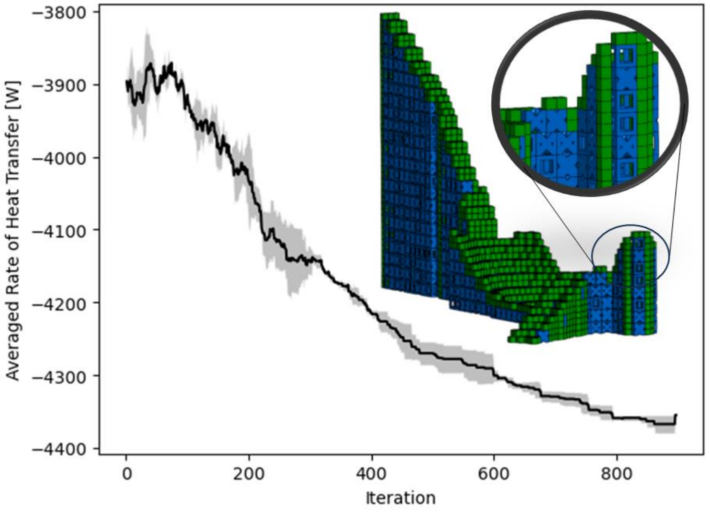

	$\lvert Q_{out} \rvert$	V(x)	P-norm Stress	$Max(U_z)$ [μm]	SC/TR/FC	V(x) < 4570 P-norm < 0.66 $Max(U_z)$< 66
Solid	6470	7617	0.053	4.6	--	No
SC Only	3182	3711	0.166	19.45	631/0/0	No
TR Only	3756	4468	0.108	13.07	0/631/0	No
FC Only	4775	4891	0.072	8.08	0/0/631	No
$Op_{avg,3}$	4365 (10.5)	4481 (11.2)	0.11 (0.00094)	12.95 (0.226)	175/197/259 (29.3/14.8/37.8)	Yes

Case Study of Heat Exchanger Adapter: Validation

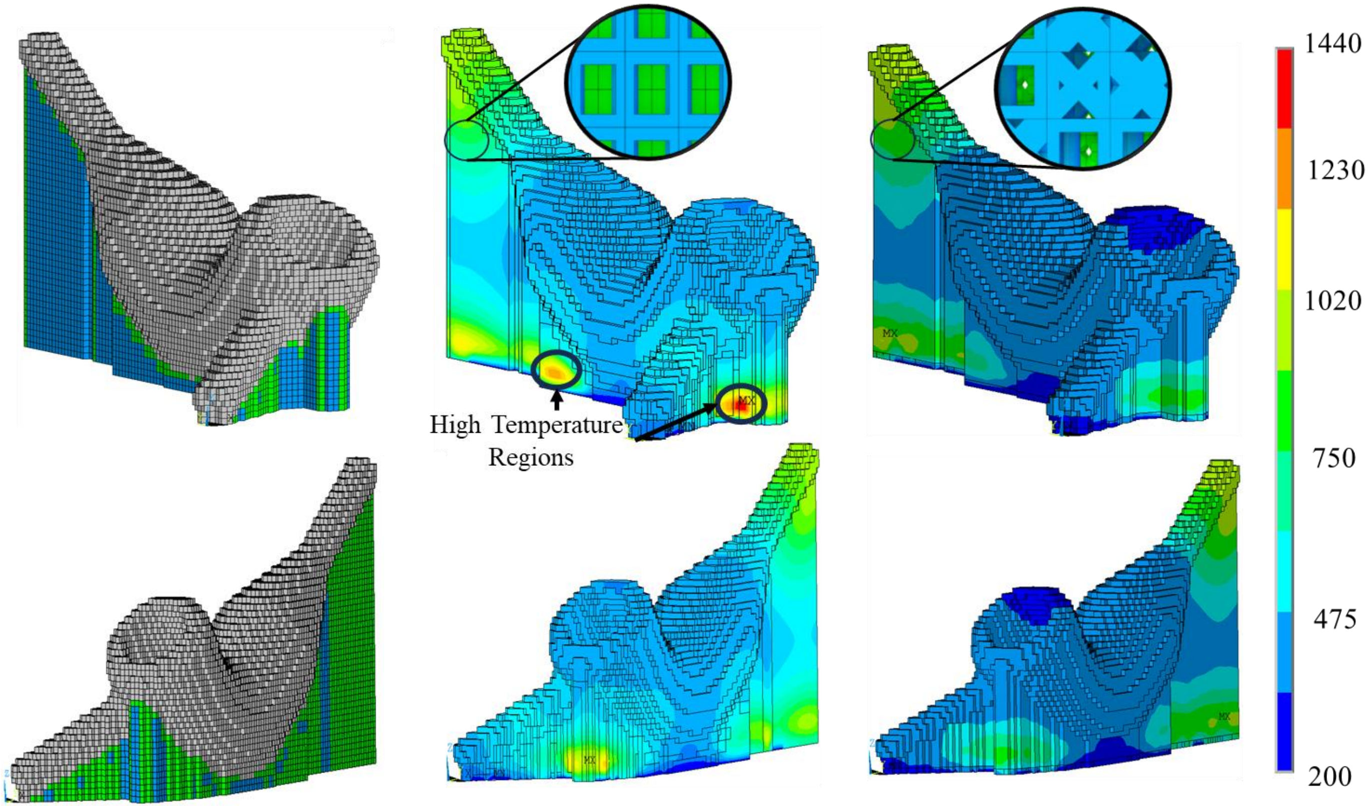

Average of ~32% Heat dissipation

No change in deformation in Z

Future Work

Evaluating Other Priority Factors

Lattice Printability
- Defects
- Transition

Time
- Dissipation Time
- Build time

Guidelines for User-Defined Constraints

Pre-defined unit cell library

Stage-dependent annealing swapping strategy

Additional Validation

Computational
- Gradient Based Optimizers
- Non-Gradient based optimizers

Physical Structure
- Calibrating ISM

36. Liu et. al 2020

Physical Validation: Calibration

Haynes 282[34]

- Nickel-based superalloy
  - High strength
  - Resistance to corrosion and oxidation
  - Good creep and fatigue performance
- Applications
  - Industrial gas turbines
  - Powerplant parts

Thermo-mechanical Model[33]

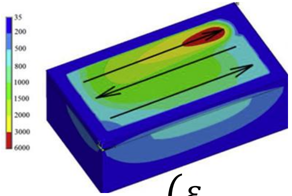

$$\varepsilon_0^{inh} = \begin{cases} \varepsilon_{xx} \\ \varepsilon_{yy} \\ \varepsilon_{zz} \end{cases}$$

Experimental Results*[35,36]

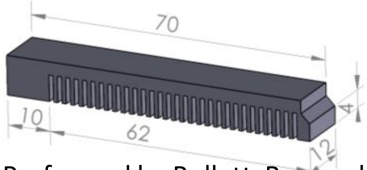

*Performed by Rollett Research Lab

Regression Model[34]

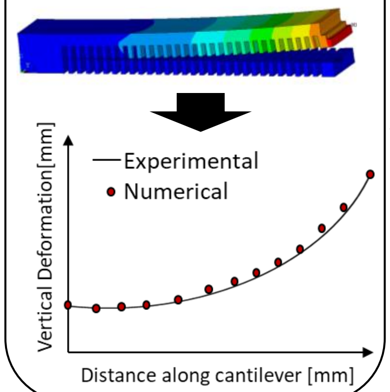

$$\varepsilon^{inh} = \begin{cases} \varepsilon_{xx} \\ \varepsilon_{yy} \\ \varepsilon_{zz} \end{cases}$$

33. Chen, Q., et. al (2019) 34. Shaikh, A.S., et. al (2021) 35. Miki, T., and Yamada, T. (2021) 36. Setien, I., et. al (2019)

Curve Fitting Regression Model Flowchart

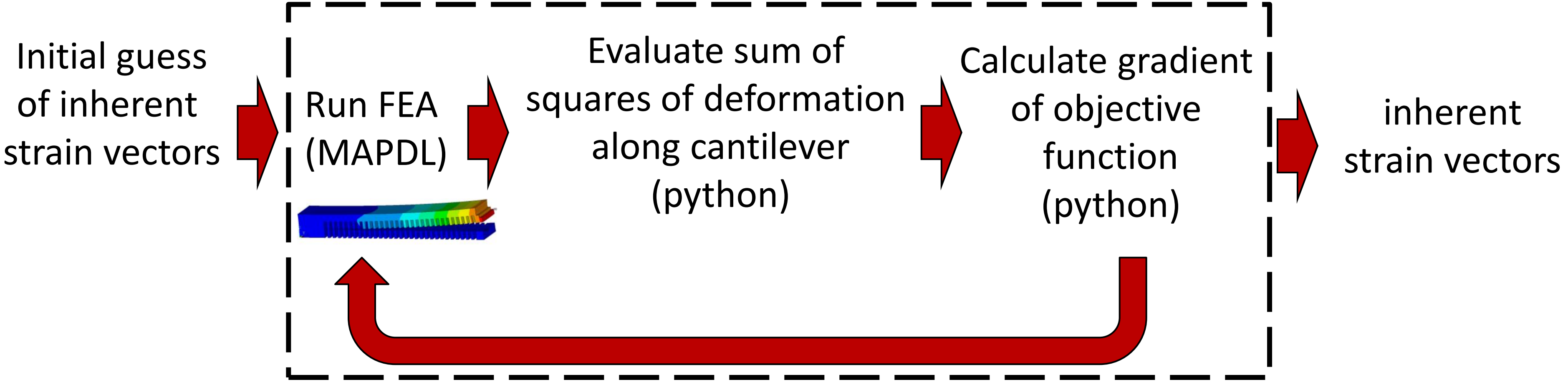

Mechanical Ansys Parametric Design Language (MAPDL)

- Scripting language used to interact with the ANSYS mechanical solver

Python code: scipy.optimize.least_squares

- Solves a nonlinear least-squares problem with bounds on the variables

Physical Validation

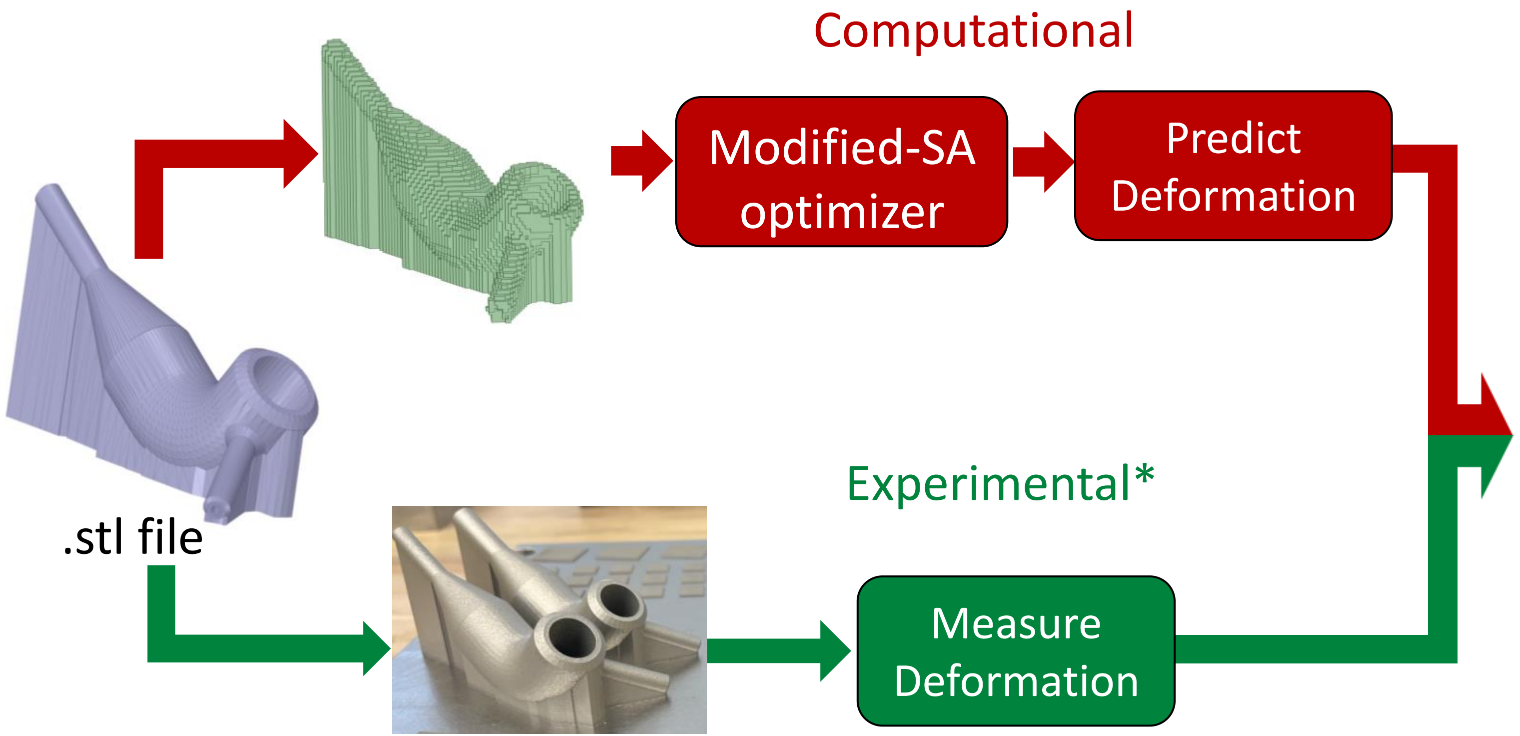

Image by Rollett Research Lab

$$\sqrt{\frac{\sum(U_c - U_E)^2}{N}}$$

*Performed by Rollett Research Lab

Printability of Lattice Structure [22]

Material Dependency

- Porosity
- Residual stress

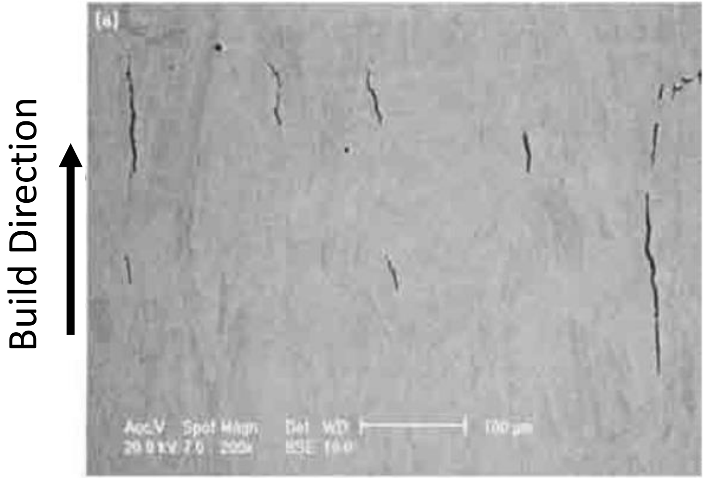

Cracking found in nickel-based superalloy [34]

Geometric Dependency

- Strut Diameter
- Strut Orientation

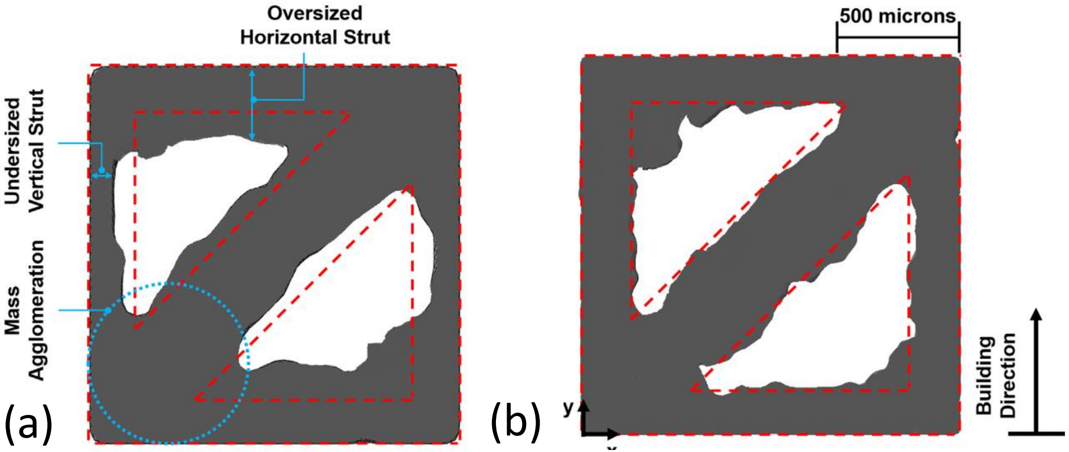

2D reconstruction of initial design of unit cell (dashed lines) with (a) as-printed and (b) compensation[35]

Printability of Lattice Structure: Defects[22]

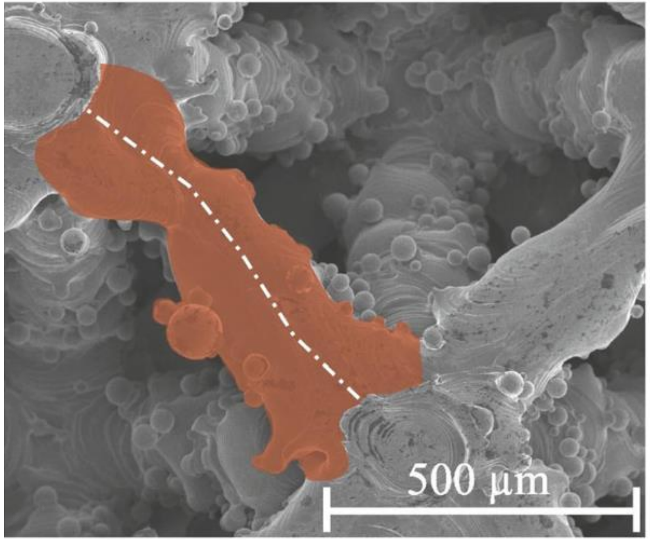

Surface roughness

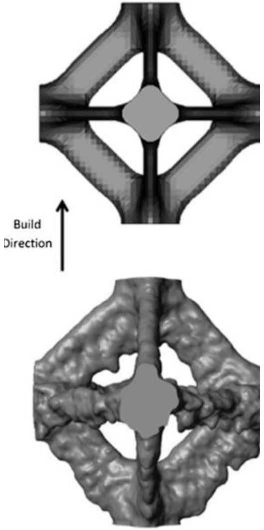

Upskin vs Downskin

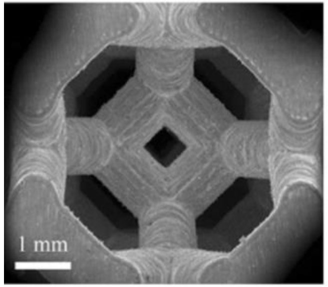

Stair-stepping

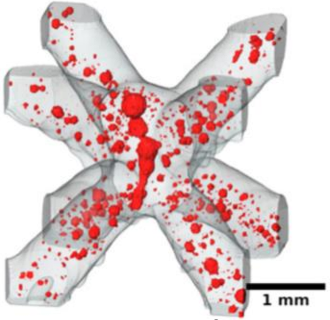

Porosity

22. Echeta, I., et. al (2020)

Parameterizing Transition Subdomain

Fixed Pin Size

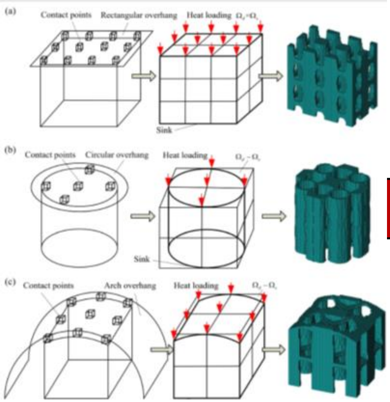

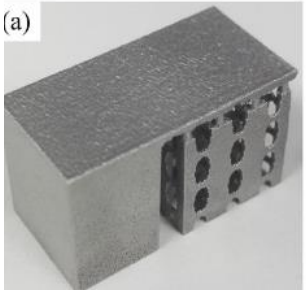

5

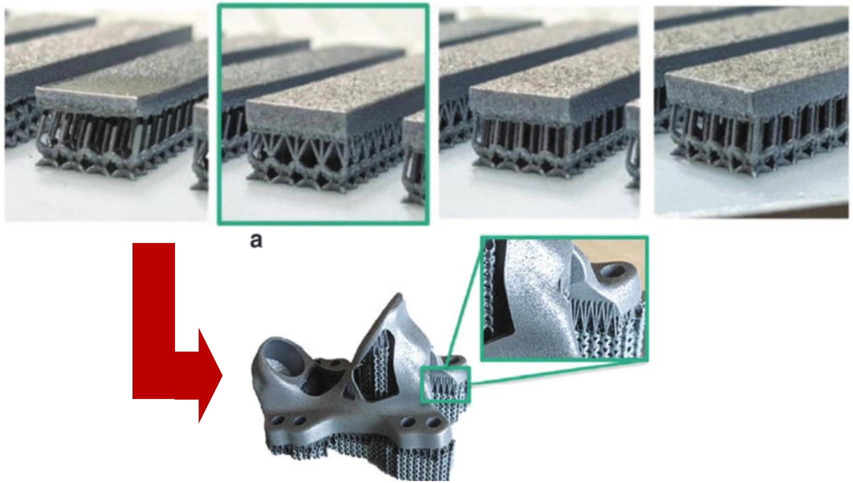

17

Variable Pin Size

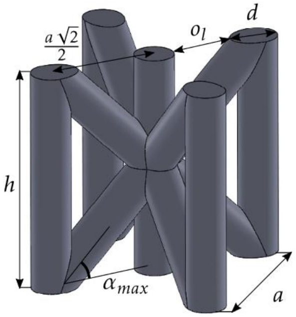

50

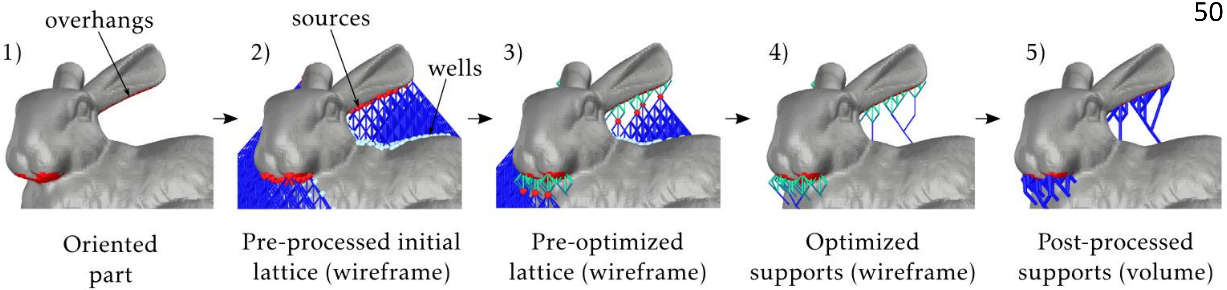

5. Huang, R., et. al (2020) 17. Boos, E., et. al (2022) 50. Vaissier, B., et. al (2019)

Parameterizing Transition Subdomain

Effect of support structure on temperature distribution[zz]

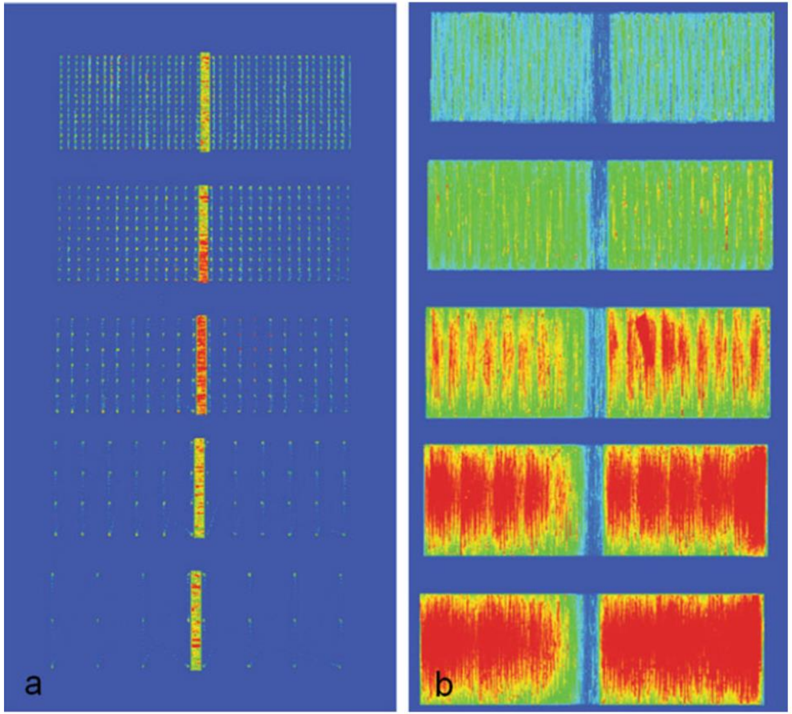

[zz] Malekipour et al. (2018)

Incorporating complex, curved structures for lattice support generation

1. Multisize unit cells[37]

2. Extended unit cell library[38]

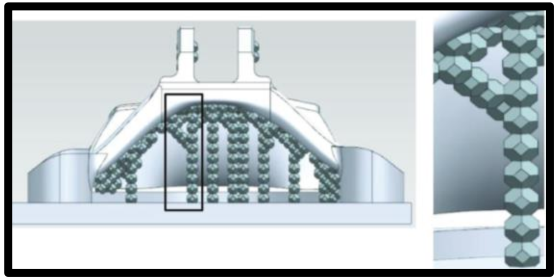

3. Forced flat domain[9,20,36]

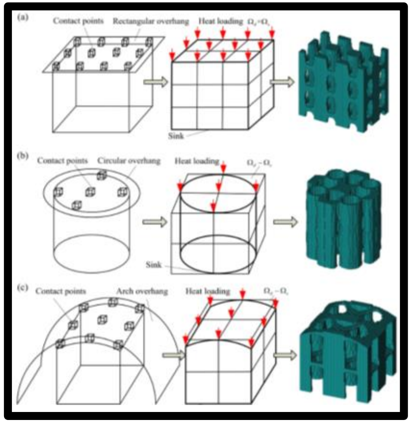

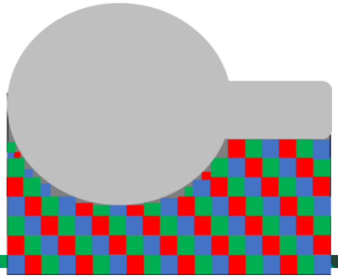

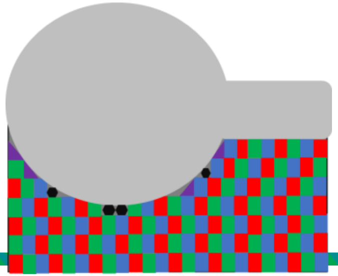

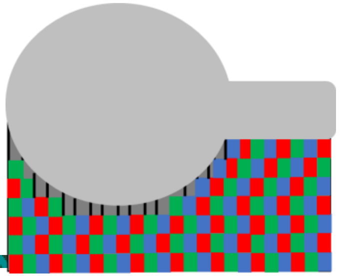

9. Huang ,R. et al. (2020) 20. Vaissier, B., et. al (2022) 37. Boos, E., et. al (2022) 38. Vaidya, R. and Anand, S. (2016)

Guidelines for Unit Cell Library: Generation

yy

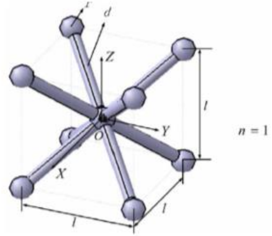

Fig. 2 Example of the final calculation result of the lattice unit

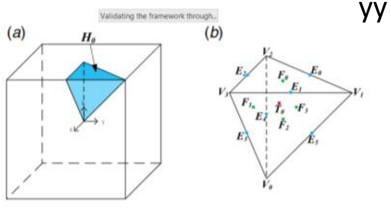

Fig. 4 The fundamental tetrahedron domain: (a) cube grid decompositions and (b) distribution of key points on the sub-tetrahedron

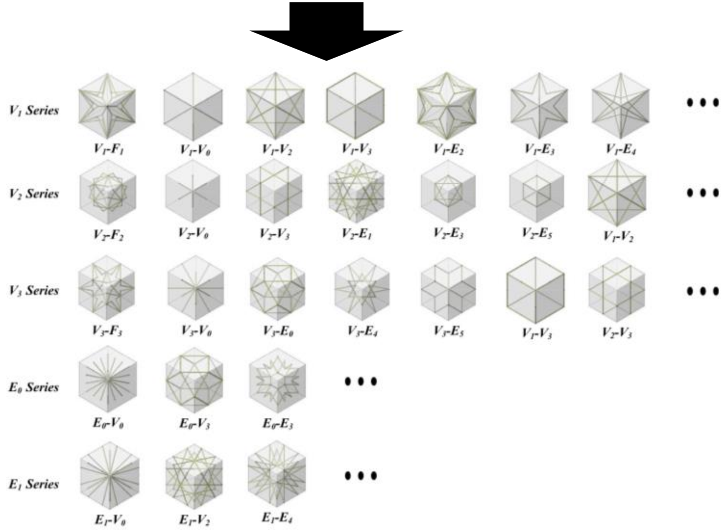

xx

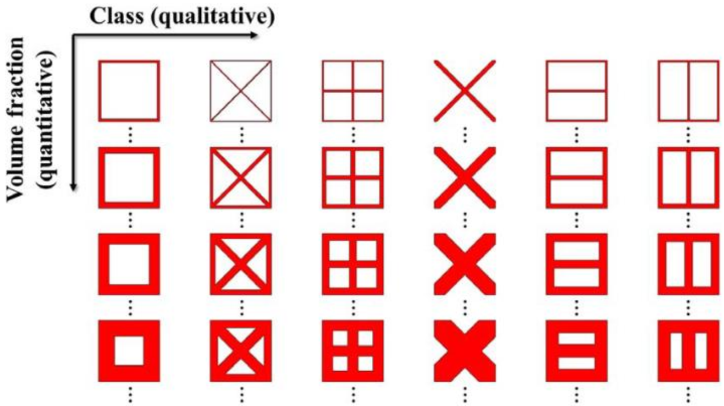

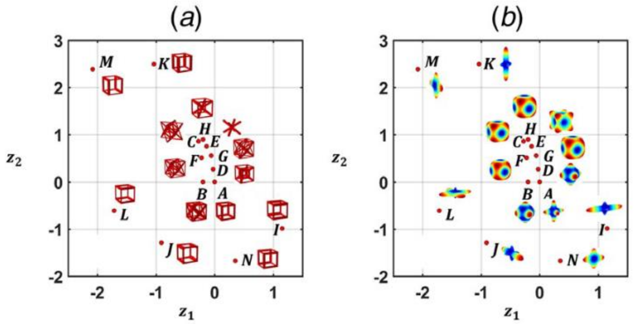

Guidelines for Unit Cell Library: Selection

Considerations:

- Connection (including Intracellular stress)
- Increased design exploration
- Priority factors
- Printing parameters

vv

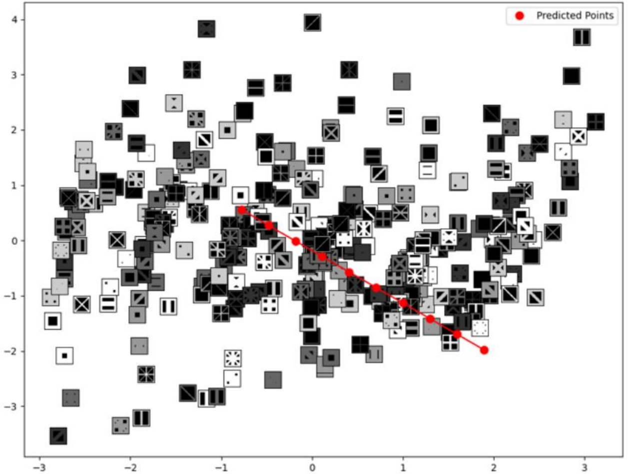

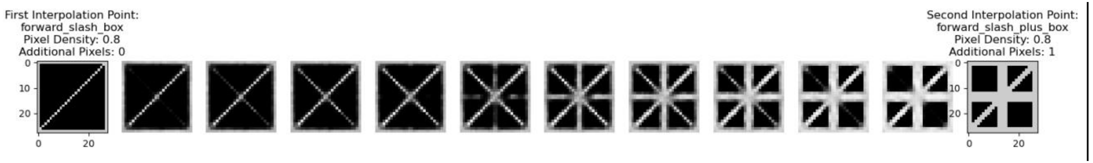

Guidelines for Stage-dependent Annealing Swapping Strategy

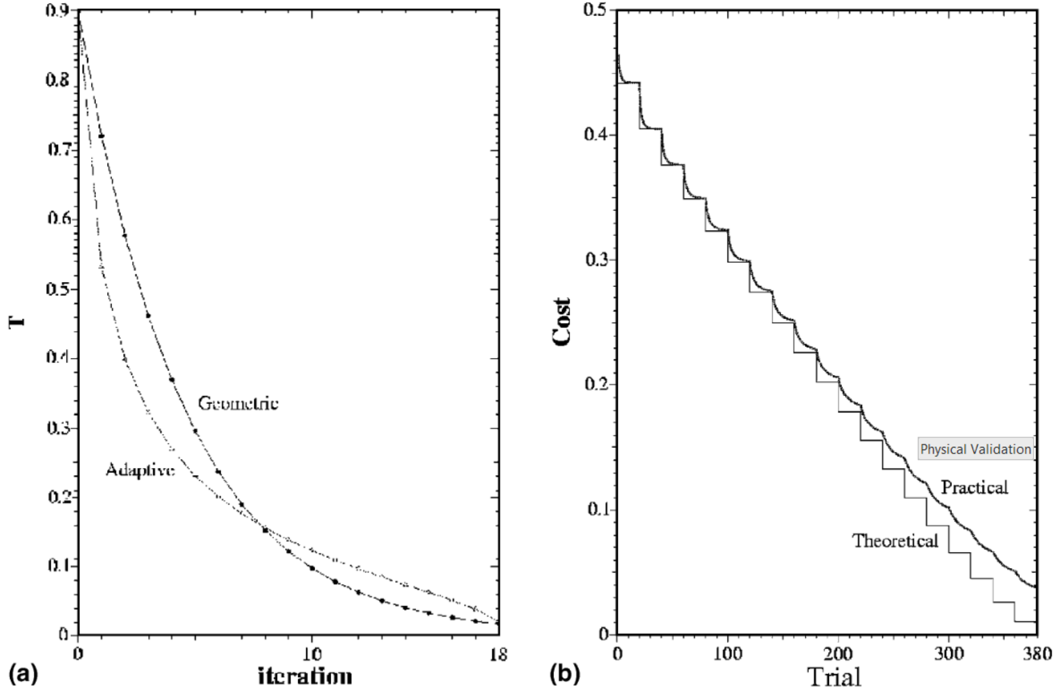

Geometric cooling schedule

$$T_{k+1} = \alpha * T'_k$$

Adaptive Cooling Schedule[51]

$$T'_{k+1} = T'_k \cdot \left(1 - T'_k \left(\frac{\Delta}{\sigma^2(T'_k)}\right)\right)$$

51. Triki, E., et al. (2005)